CASL-U-2015-0221-000

MCNPX and KENO-VI Simulations of WBNP Unit 1 with Keno Comparisons

Benchmark Results
VERA Core Physics Progression Problems 1 - 5

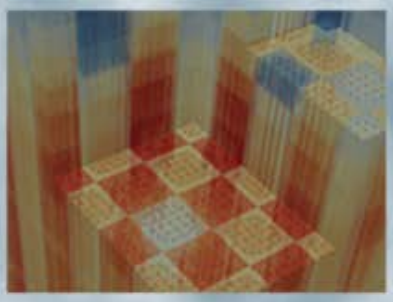

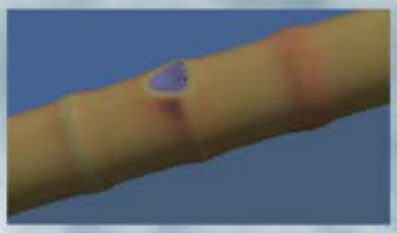

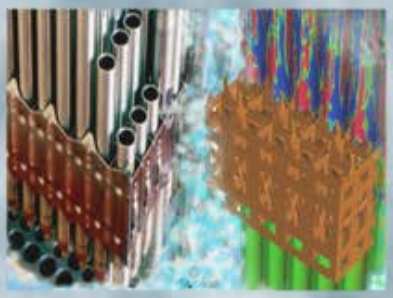

William Gurecky
Erich Schneider
The University of Texas at Austin

February 20, 2015

U.S. DEPARTMENT OF ENERGY | Nuclear Energy

REVISION LOG

Revision	Date	Affected Pages	Revision Description

Document pages that are:

Export Controlled _____None_____

IP/Proprietary/NDA Controlled_____None_____

Sensitive Controlled_____None_____

Requested Distribution:

To: Andrew Godfrey

Copy:

EXECUTIVE SUMMARY

Provided here is a comparison of the computational modeling results for the AMA Core Physics Benchmark Progression Problems 1 through 5 for MCNPX and KENO-VI. A brief summary of each problem is included as well, however a full description of each problem geometry, material specifications and operating conditions is left to Ref. [1] [CASL-U-2012-0131-003]. MCNPX version 2.7.0 was utilized to produce the benchmark results. MCNPX provides a limited set of continuous energy cross section libraries bundled with the default installation. Where necessary, NJOY 2012 was utilized to generate MCNPX compatible ACE continuous energy cross section libraries from ENDF VII.0 data available on the LANL T2 website.

CONTENTS

EXECUTIVE SUMMARY iii

CONTENTS v

FIGURES vi

TABLES ix

ACRONYMS 1

INTRODUCTION 2

Problem #1: 2D HZP BOC Pin Cell 2
RESULTS 2

Problem #2: 2D HZP BOC 17x17 Fuel Lattice 4
RESULTS 4

Problem #3: 3D HZP BOC 17x17 Fuel Lattice 12
RESULTS 12

Problem #4: 3D HZP BOC 3x3 Fuel Assembly Array 16
RESULTS 16

Problem #5: 3D HZP BOC Quarter Core 20
RESULTS 21

MISCELLANEOUS BENCHMARKS 27
Problem #4-2D: 2D HZP BOC 3x3 Assembly 27
Problem #5-2D: 2D HZP BOC Quarter Core 29

APPENDIX A 33
Problem #5 – 3D Quarter Core ITC Calculations 33

APPENDIX B 36
Pin Power Normalization 36

REFERENCES 36

FIGURES

Figure 1) Symmetric pin weights....6

Figure 2) Problem 2A (565K) CE MCNPX Pin Power Distribution Result....6

Figure 3) Problem 2B (600K) CE MCNPX Pin Power Distribution Result....7

Figure 4) Problem 2C (900K) CE MCNPX Pin Power Distribution Result....7

Figure 5) Problem 2D(1200K) CE MCNPX Pin Power Distribution Result....7

Figure 6) Problem 2E 12 Pyrex....8

Figure 7) Problem 2F 24 Pyrex....8

Figure 8) Problem 2G 24 AIC....8

Figure 9) Problem 2H 24 B4C....9

Figure 10) Problem 2I Instrument thimble....9

Figure 11) Problem 2J Instrument thimble + 24 Pyrex....9

Figure 12) Problem 2K Zoned + 24 Pyrex....10

Figure 13) Problem 2L 80 IFBA....10

Figure 14) Problem 2M 128 IFBA....10

Figure 15) Problem 2N 24 WABA + 104 IFBA....11

Figure 16) Problem 2O 12 Gadolinia....11

Figure 17) Problem 2P 24 Gadolinia....11

Figure 18) Problem 3A MCNPX vs. KENO Axial Power Distribution. Absolute percent differences shown. The 3D visualization of the MCNPX result is provided by mayavi2....13

Figure 19) Problem 3B MCNPX vs. KENO Axial Power Distribution. Absolute percent differences shown....14

Figure 20). MCNPX P3a radial pin power distribution....15

Figure 21) MCNPX P3b radial pin powers....15

Figure 22. Left: P3a radial power distribution relative percent difference map. Right: P3b radial power distribution relative percent difference map....15

Figure 23) MCNPX (blue) vs. KENO (red) Differential Rod Worth for Problem 4....18

Figure 24) MCNPX (blue) vs. KENO (red) Integral Rod Worth for Problem 4. Uncertainty bars obscured by width of plotted lines. 18

Figure 25) AMA P4 Pin power distribution. Control rods located 257.9 cm from bottom core plate. Right: Axial power distribution comparison with absolute percent difference shown. 19

Figure 26) Problem 4 167 step rod insertion assembly power plots. 20

Figure 27) Top down view of WB1 quarter core model. RCCA bank positions shown on the right. 20

Figure 28) WB1 quarter core critical configuration summary plot. 22

Figure 29. Differential rod worth curve for bank D in Watts Bar I 3D quarter core case. 23

Figure 30. Integral rod worth curve for bank D in Watts Bar I 3D quarter core. 24

Figure 31) Left) Visualization of the 3D pin power distribution. Performed with Mayavi2. Right) Radially integrated, axial power distribution comparison between MCNPX and KENO-VI. All absolute axial percent differences are below 1.0%. 25

Figure 32) Left) MCNPX Axially integrated assembly power distribution for the 3D-p5, case 1. Right) MCNPX – KENO assembly power distribution relative percent difference map. 26

Figure 33) P4-2D pin power results. Left: AIC-Controlled. Right: Uncontrolled. 27

Figure 34) Octant symmetric MCNPX vs KENO-VI Pin Power %Difference maps.P4-2D Controlled on the left, P4-2D Uncontrolled on the right. A +0.5% [MCNP – KENO] relative error gives a deep red and a -0.5% result yields a deep blue. 28

Figure 35) P5-2D pin power maps. Left: Uncontrolled case. Right: AIC controlled pin power distribution MCNPX result. Control bank D used. (Not pictured: B4C controlled pin power map). 30

Figure 36) P5-2D Assembly power weights. 30

Figure 37) AIC Controlled assembly power distribution MCNPX result with a MCNPX vs KENO relative %difference map. 31

Figure 38) MCNPX relative 1SD uncertainty in P5-2D controlled assembly powers 31

Figure 39) Uncontrolled assembly power distribution MCNPX result alongside a MCNPX vs KENO relative %difference map. 31

Figure 40) MCNPX relative 1SD uncertainty in P5-2D Uncontrolled assembly powers 32

Figure 41) B4C Controlled assembly power distribution MCNPX result with a MCNPX vs KENO relative %difference map. 32

Figure 42) MCNPX relative 1SD uncertainty in P5-2D B4C controlled assembly powers. 32

Figure 43) Moderator density only effect on keff. 34

Figure 44) Doppler broadening effect on keff. 34

Figure 45) Refined DTC result compared to previous calculation. 35

TABLES

Table 1) Problem 1 MCNPX vs. KENO k_{eff} comparison (Table P1-5, p. 21, Ref [1]). *1A 565K NJOY CE cross sections generated from ENDFVII source data.....2

Table 2) Problem 2 MCNPX vs. KENO k_{eff} comparison (Table P2-5, p. 29, Ref [1]). *2A 565K NJOY CE cross sections generated from ENDFVII source data.....5

Table 3) Problem 2 pin power MCNPX vs.....5

KENO-VI RMS differences.....5

Table 4) Problem 2 MCNPX pin power relative 1SD 5

uncertainty summary.....5

Table 5) Problem 3 MCNPX vs. KENO k_{eff} comparison (Table P3-4, p. 45, Ref [1]). *3B 565K NJOY CE cross sections generated from ENDFVII source data.....12

Table 6) Problem 3 MCNPX vs KENO Axial Power absolute RMS percent differences. 14

Table 7) Problem 3 MCNPX radial power uncertainty summary table.....15

Table 8) Problem 4 MCNPX vs. KENO k_{eff} comparison (Table P4-4, p. 53, Ref [1]). 17

Table 9) Differential Rod Worth Comparison. 17

Table 10) Problem 5 eigenvalue only results.....21

Table 11) Problem 5 ITC results.....22

Table 12) Problem 5 RCCA bank D differential rod worth comparison table. 23

Table 13) Problem 5 ZPPT rod and boron worth results. 24

Table 14) 3D pin power difference summary. 26

Table 15)MCNPX p5-3D pin power uncertainty summary.....26

Table 16) MCNPX vs KENO k_{eff} comparison for problem 4-2D.....27

Table 17) MCNPX vs KENO-VI pin power %RMS differences for Problem 4-2D.....27

Table 18) P4-2D MCNPX Pin power uncertainty summary 28

Table 19) P4-2D Uncontrolled normalized assembly powers. 28

Table 20) P4-2D Controlled normalized assembly powers. 29

Table 21) P5-2D k_{eff} Result Summary. 29

Table 22) P5-2D MCNPX Pin power uncertainty summary. 30

Table 23) Problem 5-2D Assembly power distribution relative RMS percent difference 33

Table 24) Problem 5 S(α,β) worth results.....33

Table 25) Sensitivity of the eigenvalue to thermal scattering treatment of the H1 isotope in light water.....33

Table 26) Moderator density coefficient.....34

Table 27) Doppler temperature coefficient.....35

ACRONYMS

AMA	Advanced Modeling Applications
BOC	Beginning of Cycle
CASL	Consortium for Advanced Simulation of Light Water Reactors
HZP	Hot Zero Power
LWR	light water reactor
ORNL	Oak Ridge National Laboratory
VERA	Virtual Environment for Reactor Applications

INTRODUCTION

MCNPX results were obtained using the Nukestar computing cluster at the University of Texas at Austin. Nukestar is a heterogeneous Beowulf style cluster consisting of 158 cpus @ 2.1 GHz AMD Opteron processors distributed amongst 4 machines and 56 cpus @ 1.99 GHz AMD Opteron processors distributed amongst 3 machines. Each core is accompanied by 2 GB of 1600MT/s RAM. All nodes run Ubuntu 11.04 with kernel version 2.6.38-8-server. OpenMPI version 1.4.3 is installed on all nodes. Inter-node communication is over one gigabit ethernet.

MCNPX input decks, NJOY generated cross sections and MCNPX results in the HDF5 format are available upon request. Contact William Gurecky (william.gurecky@utexas.edu) for this data. One standard deviation (SD) uncertainties are provided for all results.

PROBLEM #1: 2D HZP BOC PIN CELL

"This problem consists of a single Westinghouse 17x17-type fuel rod cell at beginning-of-life (BOL) conditions. The materials are standard for this type of reactor: UO2, Zircaloy-4, and water. The moderator also contains soluble boron as a chemical shim for maintaining criticality. The pellet-clad gap consists of helium gas, but this material may be neglected due to its insignificant neutron cross section.

This problem is divided into five calculations. The first (part A) represents typical zero power isothermal conditions which are representative of power reactor startup physics testing. Calculations B, C, and D are for the same rod geometry but with a range of fuel temperatures that are common under full power operating conditions. Problem 1E is an IFBA fuel rod." – Ref. [1].

RESULTS

Table 1 provides the computed multiplication factor for the five problem 1 scenarios for MCNPX and KENO, as well as the difference in [pcm].

Table 1) Problem 1 MCNPX vs. KENO k_{eff} comparison (Table P1-5, p. 21, Ref [1]). *1A 565K NJOY CE cross sections generated from ENDFVII source data.

Case	Moderator Temp [K]	Fuel Temp [K]	MCNPX	Std dev	KENO-VI	Std dev	Diff [pcm]
1A*	565	565	1.18680	0.00006	1.187038	0.000054	-23
1B	600	600	1.18165	0.00005	1.182149	0.000068	-50
1C	↓	900	1.17154	0.00006	1.171722	0.000072	-18
1D	↓	1200	1.16298	0.00006	1.162603	0.000071	38
1E	↓	600	0.77098	0.00005	0.771691	0.000078	-71

Problem 1A provided an opportunity to demonstrate the use of NJOY 2012 to build continuous energy, Doppler broadened cross sections from ENDF VII data at 565 Kelvin suitable for use in MCNPX.

Light water thermal scattering treatment is handled by ENDF VII incoherent elastic scatter libraries accompanying the default install of MCNPX v2.7.0.These data libraries are available for 500, 550,

and 600 Kelvin. For case 1A, the 550K ENDF VII.0 light water thermal scattering library was utilized (lwtr.15t). The k_{eff} result reported in Table 1 is not corrected to account for the temperature discrepancy present in the thermal scattering treatment. At 565 Kelvin, a light water thermal scattering temperature sensitivity of -1.186 [pcm/K] was determined by a simple linear sensitivity study.

All other materials, including bound Oxygen in uranium oxide, were subject to free-gas thermal scattering treatment. A sensitivity analysis was conducted and$S(\alpha,\beta)$ scattering treatment of uranium oxide thermal scattering was found to have a minimal impact on the solution. In this study, case 1B was repeated with thermal $S(\alpha,\beta)$ scattering treatment of Uranium oxide (ZAID o2/u.13t and u/o2.13t) and a k_{eff} of 1.18214 ± 0.00007 was found, a difference of 49 [pcm].

To quantify the impact of the ENDF-VII versus ENDF-VI cross sections, problem 1A was re-run with ENDF VI.8 cross section data. MCNPX reported 1.18339 ± 0.00005 for keff in this case. The KENO-VI problem 1A solution when using ENDF VI.8 data is given to be 1.183364 ± 0.000111, for a difference between the two codes when using ENDF-VI data of just 3 [pcm]. The change in cross section library versions is noted to have shifted both results by approximately 350-450 [pcm]. All other calculations in this report were carried out with ENDF-VII data.

The number of particles tracked and computation time for problem 1, and all other problems reported in this document, are provided. As a representative example, problem 1B was run with [kcode 1e6 1.0 75 200] on 24 processors for a total of 3900 minutes CPU time as reported by MCNPX. This corresponded to a walltime of approximately 2½ hours. Details of the KENO reference calculations are included in Ref. [1].

PROBLEM #2: 2D HZP BOC 17X17 FUEL LATTICE

"The second AMA core physics benchmark problem involves a simple two-dimensional array of fuel rods (a fuel lattice) typical of the central axial region of PWR fuel assemblies. In addition to the multiplication factor, the results also permit comparison of the normalized fission reaction rate distribution (often referred to as 'pin powers') among the fuel rods.

The problem consists of a single Westinghouse 17x17-type fuel lattice at beginning-of-life (BOL). Other materials such as silver-indium-cadmium (AIC), boron carbide (B4C), Pyrex (borosilicate glass - B2O3-SiO2), and B4C-Al2O3 are used for neutron poisons inserted into the guide tubes, and stainless steel 304 is used for the instrument tube thimble and other structural materials. Some integral burnable absorbers such as IFBA and Gadolinia are also included in some of the test cases.

This problem will be divided into several calculations. The first (part A) represents typical zero power isothermal conditions which are representative of power reactor startup physics testing. Other calculations (parts B, C, and D) are for the same geometry but with a range of fuel temperatures that are common under full power operating conditions, consistent with problem 1. Parts 2E to 2P test the capability to accurately model radial heterogeneities created by different burnable poisons. Finally, 2Q tests a code's capability to accurately model the reactivity depression and radial power distribution produced by spacer grids." -- Ref. [1].

RESULTS

Table 2 provides the computed neutron multiplication factor for the problem 2 scenarios for MCNPX and KENO, as well as the difference in [pcm]. Table 3 provides the root mean squared differences for the MCNPX and KENO computed pin powers.

Significant differences between the MCNPX and KENO results were found for scenario 2N for k_{eff}. Revisiting this scenario, it was determined that in the case of 2N, two differing specifications for the WABA neutron poison was available in Ref. [1]. However, the slight difference in composition was found to have a marginal effect on computed k_{eff} (5 [pcm]).

MCNPX version v.2.7.0 with ENDF/B VII.0 cross sections was utilized to produce these results. As a representative example, problem 2B was run with 32 processors for a total of 23450 minutes CPU time with [kcode 1e5 1.0 250 2750], corresponding to approximately 13 hours wall-time. Details of the KENO reference calculations are included in Ref. [1].

Table 2) Problem 2 MCNPX vs. KENO k_{eff} comparison (Table P2-5, p. 29, Ref [1]). *2A 565K NJOY CE cross sections generated from ENDFVII source data.

Case	Description	Cladding Temp [K]	Fuel Temp [K]	MCNPX ENDF VII.0	Std dev	KENO ENDF VII.0	Std Dev	Err [pcm]
2A*	No Poisons	565	565	1.18181	4.00E-05	1.18217	1.68E-05	-36
2B	↓	600	600	1.18284	4.00E-05	1.18336	2.40E-05	-52
2C	↓	↓	900	1.17338	4.00E-05	1.17375	2.30E-05	-37
2D	↓	↓	1200	1.16527	4.00E-05	1.16559	2.30E-05	-32
2E	12 Pyrex	↓	600	1.06929	4.00E-05	1.06963	2.40E-05	-34
2F	24 Pyrex	↓	↓	0.97577	4.00E-05	0.97602	2.60E-05	-25
2G	24 AIC	↓	↓	0.84761	4.00E-05	0.8477	2.50E-05	-9
2H	24 B4C	↓	↓	0.78822	4.00E-05	0.78822	2.50E-05	0
2I	Inst Thimble	↓	↓	1.17938	4.00E-05	1.17992	2.40E-05	-54
2J	Inst + 24 Pyrex	↓	↓	0.97506	4.00E-05	0.97519	2.50E-05	-13
2K	Zoned + 24 Pyrex	↓	↓	1.01992	4.00E-05	1.02006	2.50E-05	-14
2L	80 IFBA	↓	↓	1.01823	4.00E-05	1.01892	2.40E-05	-69
2M	128 IFBA	↓	↓	0.93808	4.00E-05	0.9388	2.50E-05	-72
2N	104 IFBA + 20 WABA	↓	↓	0.86897	4.00E-05	0.86962	2.50E-05	-65
2O	12 Gadolinia	↓	↓	1.04773	4.00E-05	1.04773	2.40E-05	0
2P	24 Gadolinia	↓	↓	0.92783	4.00E-05	0.92741	2.40E-05	42

Table 3) Problem 2 pin power MCNPX vs. KENO-VI RMS differences.

Case	RMS % Diff
2A	0.045%
2B	0.030%
2C	0.036%
2D	0.037%
2E	0.040%
2F	0.041%
2G	0.419%
2H	0.409%
2I	0.034%
2J	0.043%
2K	0.041%
2L	0.035%
2M	0.045%
2N	0.038%
2O	0.111%
2P	0.190%

Table 4) Problem 2 MCNPX pin power relative 1SD uncertainty summary.

Case	Average 1SD %Uncert	Max 1SD % Uncert	Min 1SD %Ucert
2A	0.027%	0.040%	0.021%
2B	0.026%	0.040%	0.021%
2C	0.026%	0.040%	0.021%
2D	0.026%	0.040%	0.021%
2E	0.028%	0.040%	0.021%
2F	0.030%	0.040%	0.021%
2G	0.031%	0.042%	0.028%
2H	0.032%	0.042%	0.028%
2I	0.027%	0.040%	0.021%
2J	0.030%	0.040%	0.021%
2K	0.031%	0.040%	0.028%
2L	0.029%	0.040%	0.021%
2M	0.031%	0.042%	0.021%
2N	0.031%	0.040%	0.028%
2O	0.028%	0.040%	0.021%
2P	0.030%	0.040%	0.021%

Octant symmetric pin power distributions are given in figures Figure 2 through Figure 17. The MCNPX and KENO simulations were run in quarter symmetry. The quarter symmetric pin power distributions were folded about the diagonal axis to gain a $1/\sqrt{2}$ factor reduction in the pin power uncertainties. MCNPX relative pin power uncertainty distributions are available in hdf5 format in supporting files and are summarized in Table 4. KENO-VI pin power results are available in ref.

[1]. A fixed color-scale difference map is included to highlight pin power distribution discrepancies between KENO and MCNPX. A MCNPX result of -0.5% (below the KENO result) results in a deep blue and a +0.5% pin power result relative to KENO yields a deep red. The average normalized pin power value is the average over a full 17x17 pin assembly, or equivalently, a weighted average of an octant symmetric assembly with pin weights given in Figure 1.This average is equal to 1 by definition.

0								
1	1							
1	2	1						
0	2	2	0					
1	2	2	2	1				
1	2	2	2	2	0			
0	2	2	0	2	2	1		
1	2	2	2	2	2	2	1	
1	2	2	2	2	2	2	2	1

Figure 1) Symmetric pin weights

The percent RMS difference, with KENO results taken as truth, provides a succinct measure of solution discrepancies. The RMS error may be computed by Equation (1). The RMS difference is reported alongside the percent difference maps.

$$\%RMS_{err} = \frac{100}{\sqrt{N_{pins}}}\sqrt{\sum_i w_i \Delta^2{}_i} \qquad \textbf{(1)}$$

Where Δ are the octant symmetric normalized pin power differences and w_i are the pin weights. The relative percent difference presented in the following maps is given by Equation (2). All pin power differences in this report are computed as relative differences:

$$Relative\ \%Diff = 100\ \frac{MCNPX - KENO}{KENO} \qquad \textbf{(2)}$$

MCNPX Norm Pin Pwr

1.0360	1.0082							
1.0370	1.0095	1.0098						
	1.0371	1.0389						
1.0355	1.0084	1.0110	1.0453	1.0331				
1.0328	1.0060	1.0087	1.0458	1.0514				
	1.0262	1.0280		1.0370	1.0178	0.9736		
1.0119	0.9881	0.9876	1.0115	0.9835	0.9650	0.9482	0.9384	
0.9762	0.9714	0.9713	0.9736	0.9648	0.9556	0.9462	0.9421	0.9478

avg: 1.0000 **max:** 1.0514 **min:** 0.9384

% Diff Map (UT - ORNL)

-0.03%	-0.08%							
-0.01%	0.02%	-0.05%						
	0.03%	0.03%						
0.02%	-0.05%	-0.08%	0.02%	0.17%				
0.00%	0.07%	-0.02%	0.01%	-0.01%				
	-0.05%	-0.01%		0.09%	-0.02%	0.01%		
-0.03%	0.01%	-0.04%	0.00%	-0.02%	0.01%	-0.01%	-0.05%	
-0.02%	-0.07%	-0.01%	-0.03%	0.03%	0.05%	0.05%	0.04%	0.03%

RMS Err 0.045%

Figure 2) Problem 2A (565K) CE MCNPX Pin Power Distribution Result

MCNPX Norm Pin Pwr

1.0358	1.0116							
1.0364	1.0114	1.0116						
	1.0360	1.0374						
1.0344	1.0103	1.0125	1.0422	1.0306				
1.0307	1.0066	1.0096	1.0425	1.0472				
	1.0242	1.0260		1.0326	1.0148	0.9740		
1.0098	0.9888	0.9891	1.0101	0.9837	0.9664	0.9501	0.9409	
0.9789	0.9744	0.9736	0.9751	0.9666	0.9570	0.9477	0.9431	0.9472

avg: 1.0000 **max:** 1.0472 **min:** 0.9409

% Diff Map (UT - ORNL)

0.03%	0.03%							
0.01%	0.01%	-0.04%						
	0.01%	0.01%						
0.06%	0.04%	0.01%	-0.02%	-0.03%				
-0.02%	0.00%	0.01%	-0.03%	-0.02%				
	-0.02%	0.03%		-0.01%	0.02%	-0.05%		
-0.04%	-0.05%	-0.02%	0.02%	-0.02%	-0.02%	-0.03%	0.03%	
0.08%	0.03%	-0.02%	-0.02%	0.04%	0.06%	0.03%	-0.04%	-0.07%

RMS Err 0.030%

Figure 3) Problem 2B (600K) CE MCNPX Pin Power Distribution Result

MCNPX Norm Pin Pwr

1.0362	1.0110							
1.0366	1.0114	1.0118						
	1.0365	1.0374						
1.0342	1.0104	1.0126	1.0431	1.0309				
1.0305	1.0064	1.0095	1.0425	1.0479				
	1.0245	1.0258		1.0327	1.0151	0.9739		
1.0099	0.9889	0.9890	1.0101	0.9831	0.9657	0.9499	0.9409	
0.9781	0.9742	0.9735	0.9757	0.9659	0.9568	0.9475	0.9431	0.9476

avg: 1.0000 **max:** 1.0479 **min:** 0.9409

% Diff Map (UT - ORNL)

0.05%	0.01%							
0.02%	0.01%	-0.06%						
	0.01%	-0.01%						
-0.03%	0.02%	0.02%	0.08%	0.03%				
0.00%	-0.02%	0.00%	-0.01%	0.05%				
	-0.03%	-0.01%		0.03%	0.01%	0.00%		
-0.03%	-0.02%	-0.01%	-0.01%	-0.09%	-0.08%	0.05%	-0.02%	
-0.01%	0.00%	-0.04%	0.04%	0.01%	0.04%	-0.01%	-0.02%	0.00%

RMS Err 0.036%

Figure 4) Problem 2C (900K) CE MCNPX Pin Power Distribution Result

MCNPX Norm Pin Pwr

1.0355	1.0109							
1.0363	1.0113	1.0122						
	1.0363	1.0379						
1.0350	1.0100	1.0116	1.0430	1.0306				
1.0311	1.0066	1.0094	1.0426	1.0476				
	1.0249	1.0263		1.0329	1.0147	0.9736		
1.0113	0.9889	0.9893	1.0101	0.9838	0.9655	0.9495	0.9405	
0.9784	0.9743	0.9742	0.9755	0.9662	0.9562	0.9475	0.9428	0.9472

avg: 1.0000 **max:** 1.0476 **min:** 0.9405

% Diff Map (UT - ORNL)

-0.05%	-0.05%							
-0.01%	-0.06%	-0.01%						
	-0.01%	0.00%						
0.07%	0.00%	-0.06%	0.04%	-0.07%				
0.05%	-0.01%	-0.03%	0.06%	0.02%				
	0.06%	0.05%		0.02%	-0.01%	-0.06%		
0.02%	-0.06%	0.01%	0.01%	0.01%	-0.02%	-0.05%	0.01%	
-0.01%	0.03%	0.04%	0.03%	-0.02%	-0.04%	0.01%	0.02%	-0.05%

RMS Err 0.037%

Figure 5) Problem 2D (1200K) CE MCNPX Pin Power Distribution Result

MCNPX Norm Pin Pwr

1.0174	0.9921							
0.9304	0.9637	0.9963						
	0.9332	1.0249						
0.9350	0.9693	1.0028	1.0366	1.0287				
1.0291	1.0035	0.9753	0.9521	1.0228				
	1.0353	0.9427		0.9578	1.0425	1.0312		
1.0588	1.0219	0.9764	0.9350	0.9786	1.0143	1.0242	1.0292	
1.0356	1.0234	1.0056	0.9932	1.0053	1.0211	1.0314	1.0396	1.0516

avg: 1.000 **max:** 1.0588 **min:** 0.9304

% Diff Map (UT - ORNL)

0.04%	-0.10%							
0.05%	0.02%	0.00%						
	0.00%	-0.01%						
0.03%	-0.02%	0.06%	0.04%	-0.03%				
0.01%	0.01%	0.02%	-0.02%	0.02%				
	0.03%	0.09%		-0.01%	0.00%	-0.02%		
0.10%	-0.03%	0.01%	-0.05%	-0.01%	-0.03%	-0.04%	0.02%	
0.10%	-0.04%	0.01%	-0.07%	-0.01%	-0.07%	0.00%	-0.02%	0.03%

RMS Err 0.040%

Figure 6) Problem 2E 12 Pyrex

MCNPX Norm Pin Pwr

1.0783	1.0433							
0.9715	0.9912	0.9729						
	0.9329	0.9265						
0.9255	0.9590	0.9548	0.9117	0.9267				
0.9278	0.9618	0.9578	0.9120	0.9067				
	0.9417	0.9409		0.9353	0.9672	1.0338		
0.9738	1.0042	1.0053	0.9792	1.0192	1.0505	1.0833	1.1102	
1.0476	1.0525	1.0552	1.0556	1.0725	1.0920	1.1140	1.1339	1.1546

avg: 1.0000 **max:** 1.1546 **min:** 0.9067

% Diff Map (UT - ORNL)

0.00%	0.05%							
0.01%	0.05%	-0.06%						
	-0.03%	0.03%						
-0.03%	-0.01%	0.06%	-0.01%	0.04%				
-0.02%	0.01%	-0.09%	-0.07%	-0.02%				
	-0.03%	-0.03%		0.04%	0.03%	-0.02%		
-0.06%	-0.04%	-0.07%	-0.01%	0.00%	0.03%	0.02%	0.07%	
0.04%	-0.03%	0.01%	0.05%	0.08%	-0.03%	0.02%	-0.01%	0.05%

RMS Err 0.041%

Figure 7) Problem 2F 24 Pyrex

MCNPX Norm Pin Pwr

1.0720	1.0339							
0.9419	0.9665	0.9417						
	0.8897	0.8809						
0.8772	0.9218	0.9162	0.8585	0.8767				
0.8831	0.9287	0.9230	0.8613	0.8569				
	0.9115	0.9116		0.9114	0.9674	1.0684		
0.9661	1.0057	1.0095	0.9800	1.0378	1.0913	1.1461	1.1929	
1.0682	1.0771	1.0827	1.0870	1.1160	1.1521	1.1923	1.2277	1.2566

avg: 1.0000 **max:** 1.2566 **min:** 0.8569

% Diff Map (MCNP - KENO)

-0.11%	-0.13%							
0.28%	0.05%	0.07%						
	0.48%	0.53%						
0.42%	0.20%	0.26%	0.65%	0.55%				
0.53%	0.15%	0.19%	0.62%	0.73%				
	0.35%	0.49%		0.49%	0.29%	-0.21%		
0.16%	-0.01%	-0.03%	0.23%	-0.15%	-0.28%	-0.56%	-0.59%	
-0.23%	-0.29%	-0.29%	-0.26%	-0.37%	-0.55%	-0.68%	-0.70%	-0.79%

RMS Err 0.419%

Figure 8) Problem 2G 24 AIC

MCNPX Norm Pin Pwr

1.0591	1.0192							
0.9252	0.9493	0.9232						
	0.8688	0.8587						
0.8556	0.9017	0.8955	0.8360	0.8550				
0.8633	0.9108	0.9052	0.8414	0.8399				
	0.8994	0.8999		0.9067	0.9739	1.0874		
0.9631	1.0042	1.0101	0.9825	1.0482	1.1112	1.1773	1.2342	
1.0722	1.0832	1.0908	1.0990	1.1356	1.1816	1.2316	1.2741	1.3088

avg: 1.0000 **max:** 1.3088 **min:** 0.8360

% Diff Map (UT - ORNL)

-0.14%	-0.22%							
0.33%	0.13%	0.24%						
	0.48%	0.47%						
0.48%	0.18%	0.27%	0.58%	0.46%				
0.51%	0.17%	0.22%	0.63%	0.66%				
	0.46%	0.42%		0.50%	0.33%	-0.29%		
0.24%	0.01%	-0.03%	0.24%	-0.13%	-0.29%	-0.57%	-0.60%	
-0.27%	-0.27%	-0.32%	-0.26%	-0.43%	-0.47%	-0.54%	-0.69%	-0.76%

RMS Err 0.409%

Figure 9) Problem 2H 24 B4C

MCNPX Norm Pin Pwr

1.0047	0.9925							
1.0258	1.0027	1.0067						
	1.0336	1.0368						
1.0351	1.0088	1.0115	1.0451	1.0329				
1.0326	1.0070	1.0096	1.0460	1.0517				
	1.0274	1.0289		1.0369	1.0187	0.9755		
1.0134	0.9904	0.9901	1.0129	0.9853	0.9676	0.9511	0.9413	
0.9792	0.9751	0.9741	0.9760	0.9673	0.9578	0.9488	0.9442	0.9497

avg: 0.9999 **max:** 1.0517 **min:** 0.9413

% Diff Map (UT - ORNL)

0.03%	-0.04%							
0.07%	0.04%	-0.07%						
	0.02%	0.02%						
-0.01%	0.00%	-0.02%	0.01%	0.02%				
-0.01%	0.00%	-0.06%	0.03%	0.02%				
	0.05%	0.02%		-0.01%	-0.02%	0.00%		
0.06%	0.05%	-0.03%	0.01%	-0.04%	-0.03%	-0.02%	-0.02%	
0.01%	0.03%	-0.07%	0.01%	-0.06%	0.05%	0.01%	-0.02%	-0.04%

RMS Err 0.034%

Figure 10) Problem 2I Instrument thimble

MCNPX Norm Pin Pwr

1.0405	1.0225							
0.9601	0.9827	0.9692						
	0.9306	0.9251						
0.9252	0.9587	0.9556	0.9130	0.9284				
0.9295	0.9623	0.9596	0.9141	0.9085				
	0.9433	0.9426		0.9366	0.9689	1.0361		
0.9753	1.0063	1.0078	0.9814	1.0213	1.0530	1.0846	1.1117	
1.0489	1.0554	1.0579	1.0579	1.0745	1.0945	1.1160	1.1361	1.1557

avg: 1.0000 **max:** 1.1557 **min:** 0.9085

% Diff Map (UT - ORNL)

-0.10%	-0.01%							
0.11%	0.04%	0.09%						
	0.01%	0.02%						
-0.10%	-0.03%	0.00%	0.01%	-0.04%				
0.07%	-0.07%	0.01%	-0.02%	-0.01%				
	0.05%	-0.03%		-0.05%	-0.07%	0.03%		
-0.08%	0.03%	0.01%	0.09%	0.00%	0.01%	-0.03%	-0.03%	
0.00%	-0.01%	0.02%	0.01%	0.01%	0.03%	0.00%	-0.01%	-0.02%

RMS Err 0.043%

Figure 11) Problem 2J Instrument thimble + 24 Pyrex

MCNPX Norm Pin Pwr

0.9765	1.0634							
0.9903	1.0058	0.9853						
	0.9458	0.9390						
0.9380	0.9693	0.9648	0.9238	0.9390				
0.9388	0.9711	0.9677	0.9248	0.9198				
	0.9517	0.9509		0.9477	0.9806	1.0502		
0.9813	1.0102	1.0114	0.9877	1.0284	1.0643	1.1070	1.0152	
1.0524	1.0574	1.0600	1.0622	1.0813	1.1094	1.0139	1.0445	1.0688

avg: 1.0000 **max:** 1.1094 **min:** 0.9198

% Diff Map (UT - ORNL)

-0.01%	-0.03%							
0.03%	0.03%	0.04%						
	0.03%	0.02%						
0.00%	0.04%	0.04%	0.01%	0.02%				
0.00%	0.04%	0.04%	0.03%	0.03%				
	0.08%	0.04%		0.01%	-0.01%	0.07%		
0.02%	-0.03%	-0.08%	0.03%	-0.01%	-0.03%	-0.03%	-0.07%	
0.00%	-0.04%	-0.08%	0.01%	0.00%	-0.04%	-0.08%	-0.07%	0.01%

RMS Err 0.041%

Figure 12) Problem 2K Zoned + 24 Pyrex

MCNPX Norm Pin Pwr

0.9497	0.9971							
1.0328	1.0004	0.9313						
	0.9561	1.0290						
0.9601	1.0097	1.0108	0.9412	0.9817				
1.0471	1.0217	1.0156	0.9400	0.9387				
	0.9689	1.0463		0.9539	1.0336	0.9391		
0.9646	1.0195	1.0273	0.9655	1.0148	1.0229	1.0095	1.0078	
1.0309	1.0361	1.0373	1.0302	1.0338	1.0353	1.0261	1.0023	0.9047

avg: 0.9999 **max:** 1.0471 **min:** 0.9047

% Diff Map (UT - ORNL)

0.14%	0.01%							
0.02%	0.01%	0.06%						
	0.02%	0.01%						
0.00%	0.05%	0.00%	0.04%	-0.02%				
-0.06%	0.00%	-0.06%	0.00%	-0.04%				
	-0.04%	-0.01%		-0.03%	0.05%	-0.01%		
0.04%	-0.01%	-0.03%	0.04%	-0.06%	-0.01%	0.00%	-0.01%	
0.03%	-0.03%	0.01%	-0.03%	-0.01%	0.02%	0.02%	-0.01%	0.00%

RMS Err 0.035%

Figure 13) Problem 2L 80 IFBA

MCNPX Norm Pin Pwr

0.9835	1.0396							
0.9835	1.0391	1.0389						
	0.9834	0.9831						
0.9822	1.0374	1.0360	0.9764	1.0211				
0.9814	1.0361	1.0345	0.9711	0.9695				
	0.9764	0.9784		0.9696	0.9661	1.0039		
0.9731	1.0192	1.0308	0.9790	1.0172	1.0163	0.9439	1.0146	
1.0080	0.9431	1.0337	1.0293	0.9469	1.0317	1.0361	1.0298	0.9423

avg: 1.0000 **max:** 1.0396 **min:** 0.9423

% Diff Map (MCNP - KENO)

0.03%	0.07%							
-0.11%	-0.02%	0.01%						
	0.01%	0.07%						
-0.07%	0.04%	-0.01%	0.04%	0.05%				
0.00%	0.00%	0.02%	-0.04%	-0.01%				
	-0.05%	0.06%		0.01%	0.01%	-0.04%		
0.03%	0.00%	0.10%	-0.02%	0.02%	-0.07%	-0.02%	-0.06%	
0.01%	-0.01%	0.03%	0.04%	-0.04%	-0.07%	0.00%	-0.08%	0.00%

RMS Err 0.045%

Figure 14) Problem 2M 128 IFBA

MCNPX Norm Pin Pwr

0.9756	1.0261							
0.8990	0.9963	1.0219						
	0.8922	0.9660						
0.8697	0.9720	1.0056	0.9465	0.9548				
0.8677	0.9640	0.9698	0.8648	0.8462				
	0.8816	0.8832		0.8704	0.9111	1.0549		
0.9240	1.0155	1.0180	0.9319	1.0364	1.0828	1.1280	1.1543	
1.0813	1.0931	1.0958	1.0926	1.1187	1.1460	1.1668	1.1601	1.0596

avg: 0.9986 **max:** 1.1668 **min:** 0.8462

% Diff Map (UT - ORNL)

-0.01%	0.02%							
-0.03%	0.00%	0.09%						
	0.00%	0.03%						
0.00%	-0.01%	-0.01%	-0.03%	-0.10%				
-0.02%	-0.04%	-0.02%	-0.03%	-0.06%				
	-0.03%	0.01%		-0.01%	0.00%	-0.04%		
-0.08%	0.00%	0.00%	0.01%	-0.03%	0.03%	0.07%	0.04%	
0.12%	0.03%	-0.04%	0.02%	0.03%	0.01%	0.05%	-0.01%	-0.07%

RMS Err 0.038%

Figure 15) Problem 2N 24 WABA + 104 IFBA

MCNPX Norm Pin Pwr

1.1050	1.0701							
1.0889	1.0505	1.0189						
	1.0409	0.9808						
1.0484	0.9659	0.2165	0.9881	1.0366				
1.0726	1.0228	0.9772	1.0551	1.0815				
	1.0924	1.0825		1.0789	0.9933	0.2162		
1.1047	1.0778	1.0727	1.0923	1.0478	0.9928	0.9250	0.9638	
1.0766	1.0719	1.0672	1.0639	1.0435	1.0164	0.9931	0.9997	1.0170

avg: 1.0000 **max:** 1.1050 **min:** 0.2162

% Diff Map (UT - ORNL)

0.02%	-0.08%							
0.00%	0.03%	0.09%						
	0.01%	0.03%						
0.06%	0.02%	-0.49%	-0.01%	-0.01%				
0.00%	0.04%	0.00%	-0.03%	0.03%				
	-0.02%	0.01%		0.01%	0.02%	-0.50%		
-0.05%	-0.01%	0.05%	0.05%	0.01%	-0.03%	-0.04%	-0.04%	
-0.05%	0.04%	-0.05%	0.02%	0.06%	-0.03%	-0.04%	0.01%	0.07%

RMS Err 0.111%

Figure 16) Problem 2O 12 Gadolinia

MCNPX Norm Pin Pwr

1.1679	1.1103							
1.1416	1.0534	0.2426						
	1.1171	1.0639						
1.0659	1.0825	1.0879	1.0633	0.2427				
0.2445	1.0405	1.0956	1.1095	1.0608				
	1.1145	1.1066		1.0815	1.0382	0.2414		
1.1475	1.1086	1.0328	0.2426	1.0074	1.0410	1.0055	1.0610	
1.1334	1.1147	1.0637	0.9956	1.0439	1.0758	1.0828	1.1057	1.1300

avg: 1.0000 **max:** 1.1679 **min:** 0.2414

% Diff Map (UT - ORNL)

-0.08%	-0.11%							
0.04%	0.04%	-0.66%						
	-0.09%	0.03%						
0.00%	0.04%	-0.01%	0.06%	-0.64%				
-0.56%	0.04%	0.06%	0.06%	-0.01%				
	-0.02%	-0.03%		0.08%	0.04%	-0.67%		
0.00%	-0.02%	-0.04%	-0.56%	-0.04%	0.04%	0.04%	0.02%	
-0.03%	0.03%	-0.04%	0.03%	0.01%	0.07%	0.07%	0.06%	0.00%

RMS Err 0.190%

Figure 17) Problem 2P 24 Gadolinia

PROBLEM #3: 3D HZP BOC 17X17 FUEL LATTICE

"Successful completion of this benchmark demonstrates the capability to predict the eigenvalue and pin power distribution without thermal hydraulic feedback or depletion. The problem consists of a single Westinghouse 17x17-type fuel assembly at beginning-of-life (BOL) and Hot Zero Power (HZP) isothermal conditions, based on the WBN1 data. The materials are standard for this type of reactor: UO2 fuel, Zircaloy-4 cladding, Inconel-718, Stainless Steel Type 304, and water. The moderator also contains soluble boron as a chemical shim for maintaining criticality. The focus of this problem is to demonstrate resolution of spacer grid effects on the neutron flux, and to begin modeling the non-fuel structural materials above and below the fuel stack with corresponding boundary conditions.

The assembly problem represents the first three dimensional problem in the progression of capability and requires definition of axial neutron reflector regions in conjunction with non-reentrant boundaries (vacuum). Radially, the assembly can be treated in quarter symmetry with reflection as was done for Problem 2.

The problem is divided into two calculations which differ in terms of fuel enrichment, coolant temperature, boron concentration, and the presence or absence of pyrex burnable poison." -- Ref. [1]. Problem 3A was run at a moderator and fuel temperature of 600K. Problem 3B was run at a moderator and fuel temperature of 565K. Further information can be found in Ref. [1]. Problem 3B considers a fuel assembly with the presence of Pyrex rods inserted into the guide tubes. Problem 3A does not include Pyrex rods.

RESULTS

Table 5 provides the computed multiplication factor for the problem 3 scenarios for MCNPX and KENO, as well as the difference in [pcm]. Figure 18 provides the computed axial power distribution for both MCNPX and KENO, while Table 6 provides percent differences for the MCNPX and KENO computed axial power distribution.

MCNPX version v.2.7.0 with ENDF/B VII.0 cross sections was utilized to produce these results. As an illustrative example, problem 3A was run with 140 processors for a total of 110000 minutes CPU time with [kcode 2e5 1.0 500 3750], corresponding to approximately 12 hours wall-time. Details of the KENO reference calculations are included in Ref. [1].

The MCNPX problem 3B result was corrected by -68.7 [pcm] to account for this study's use of 550K S(α, β) thermal scattering treatment of the H1 isotope. This was determined by interpolating between results obtained from MCNPX using 550 and 600K light water S(α,β) libraries.

Table 5) Problem 3 MCNPX vs. KENO k_{eff} comparison (Table P3-4, p. 45, Ref [1]). *3B 565K NJOY CE cross sections generated from ENDFVII source data.

Case	MCNPX	Std dev	KENO	Std dev	Diff [pcm]
3A	1.17525	2.00E-05	1.175722	4.90E-06	-47
3B*	1.00002	2.00E-05	1.000154	6.30E-06	-13

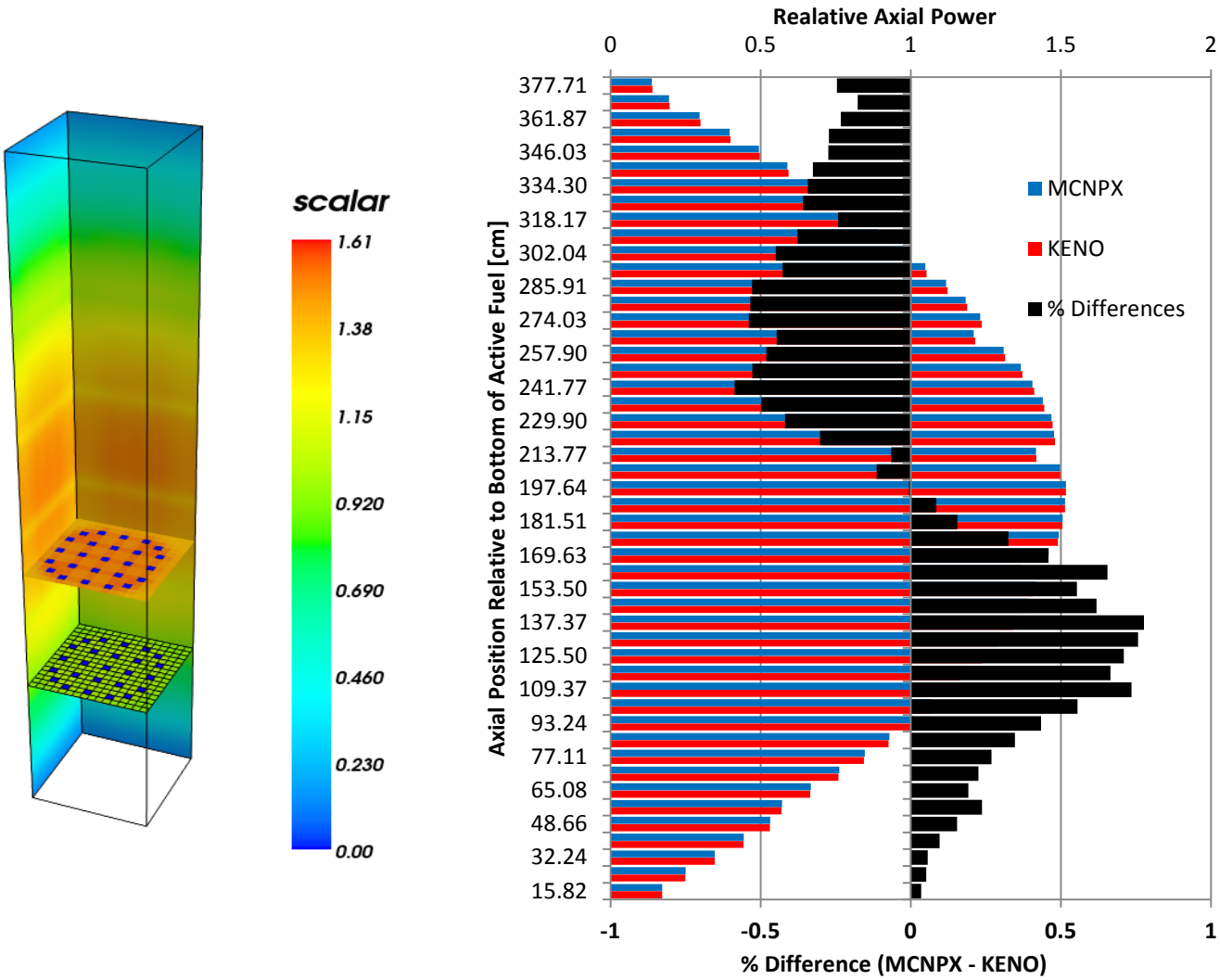

Figure 18) Problem 3A MCNPX vs. KENO Axial Power Distribution. Absolute percent differences shown. The 3D visualization of the MCNPX result is provided by mayavi2.

All axial power difference plots in this report show the **absolute** percent difference which is computed by Equation (3).

$$Absolute\ \%\,diff = 100\,(MCNPX - KENO)/KENO_{avg} \tag{3}$$

Where $KENO_{avg}$ is defined equal to one so that results are normalized against the average axial power computed by KENO. Further discussion on pin power normalization is provided in Appendix B. A relative percent difference axial power comparison yields slightly different visual shape of the difference curve due to larger relative errors where there are small axial powers.

The axial power distribution is cosine in shape with slight depressions in power where the spacer grids reside. The absolute error plotted in Figure 18 and Figure 19 exhibit shapes similar to the second harmonic of the axial power profile.

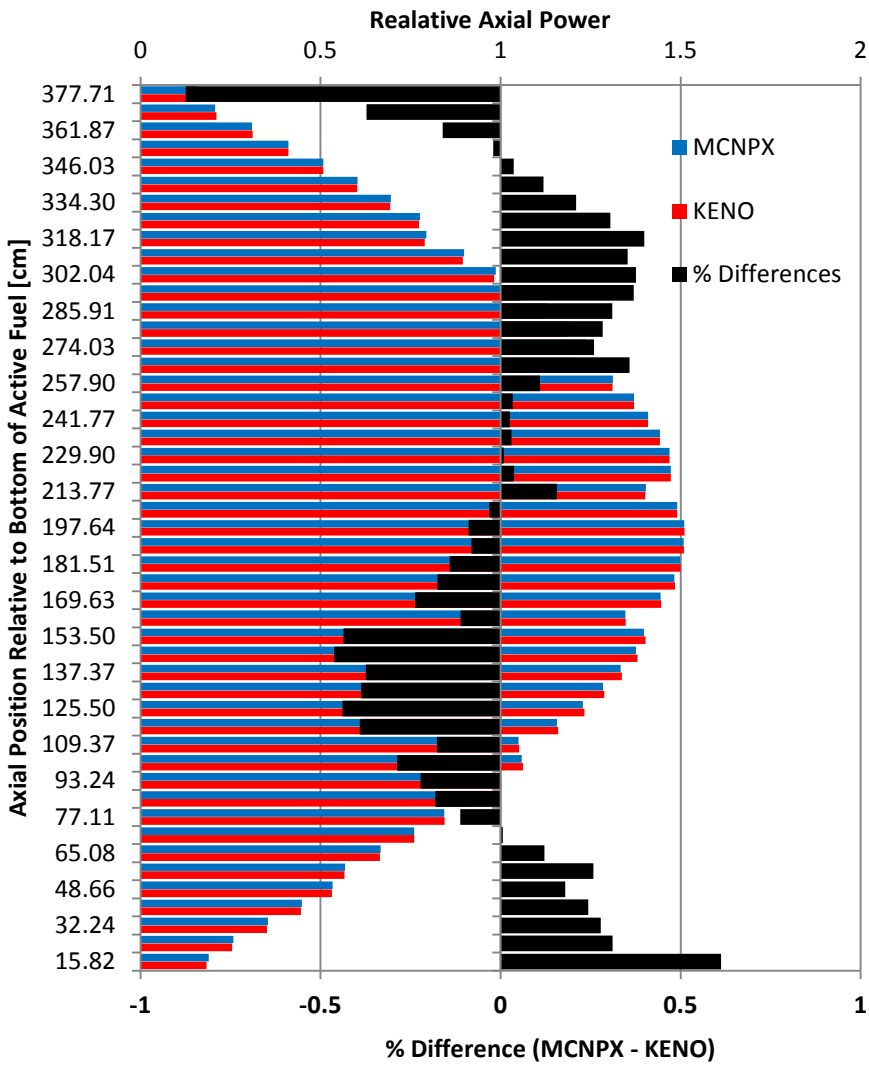

Figure 19) Problem 3B MCNPX vs. KENO Axial Power Distribution. Absolute percent differences shown.

Table 6) Problem 3 MCNPX vs KENO Axial Power absolute RMS percent differences.

Case	Absolute %RMS Difference
3A	0.421%
3B	0.279%

Radial power distribution comparisons are also made in Figure 22. The radial pin powers are axially integrated and normalized such that the radial pin powers average to 1.0 across the entire 17x17 fuel bundle.

1.0357	1.0094							
1.0360	1.0098	1.0104						
	1.0364	1.0381						
1.0348	1.0088	1.0116	1.0442	1.0319				
1.0319	1.0060	1.0094	1.0444	1.0500				
	1.0257	1.0272		1.0348	1.0165	0.9739		
1.0113	0.9885	0.9885	1.0110	0.9834	0.9654	0.9490	0.9398	
0.9770	0.9730	0.9725	0.9745	0.9655	0.9561	0.9468	0.9426	0.9482

Figure 20). MCNPX P3a radial pin power distribution.

1.0531	1.0279							
0.9587	0.9946	1.0247						
	0.9568	1.0460						
0.9591	0.9934	1.0175	1.0246	0.9646				
1.0576	1.0285	0.9850	0.9228	0.8884				
	1.0629	0.9560		0.8896	0.9076	0.9667		
1.0931	1.0538	0.9987	0.9394	0.9640	0.9850	1.0113	1.0344	
1.0720	1.0580	1.0332	1.0103	1.0125	1.0232	1.0391	1.0554	1.0732

Figure 21) MCNPX P3b radial pin powers.

Radial pin power distributions are shown in figures Figure 20 and Figure 21. The presence of the Pyrex burnable poison in problem 3B suppresses the neutron population and thus reaction rates in the surrounding pins. A MCNPX radial pin power uncertainty summary is provided in Table 7.

Table 7) Problem 3 MCNPX radial power uncertainty summary table.

Case	Average 1SD %Uncert	Max 1SD %Ucert
3A	0.090%	0.137%
3B	0.087%	0.127%

0.01%	-0.01%							
-0.02%	-0.01%	-0.02%						
	-0.01%	-0.01%						
-0.01%	-0.02%	-0.01%	0.00%	0.01%				
0.01%	0.00%	0.02%	0.00%	0.00%				
	0.02%	0.01%		-0.02%	-0.02%	0.00%		
0.01%	0.02%	0.01%	0.02%	-0.01%	-0.02%	-0.01%	0.01%	
-0.02%	0.01%	0.00%	-0.01%	0.00%	0.03%	0.01%	0.01%	0.03%

RMS Err 0.014%

0.00%	0.03%							
0.01%	0.01%	0.00%						
	0.00%	-0.02%						
0.01%	0.00%	0.02%	0.00%	-0.02%				
0.03%	0.00%	0.00%	-0.01%	0.00%				
	0.01%	-0.01%		0.02%	-0.02%	0.01%		
-0.01%	0.00%	0.00%	-0.01%	0.00%	-0.04%	0.01%	-0.04%	
0.02%	0.00%	0.01%	-0.02%	0.00%	0.01%	0.00%	0.00%	0.02%

RMS Err 0.014%

Figure 22. Left: P3a radial power distribution relative percent difference map. Right: P3b radial power distribution relative percent difference map.

Radial power distribution comparisons show excellent agreement between the two codes for both p3a and p3b cases. Radial tilt between the two codes is not seen in either case.

PROBLEM #4: 3D HZP BOC 3X3 FUEL ASSEMBLY ARRAY

"The fourth AMA core physics benchmark progression problem builds on the 3D assembly problem by the addition of multiple assemblies, RCCAs, and Pyrex burnable absorbers. Successful completion demonstrates the capability to predict the eigenvalue and pin power distribution without thermal hydraulic feedback or depletion in the presence of black neutron absorbers. Furthermore, this problem permits a detailed study of methods accuracy and convergence capability for a region of an actual reactor core, and is the first chance to perform RCCA movement and calculate a control rod reactivity worth, a critical reactor physics parameter which is often used for validation of nuclear methods.

The problem consists of nine Westinghouse 17x17-type fuel assemblies arranged in a 3x3 checkerboard pattern directly from the center of the WBN1 initial loading pattern. The fuel is at beginning-of-life (BOL) and Hot Zero Power (HZP) isothermal conditions. In addition to the same materials as Problem 3, this problem also tests the ability to define and place Pyrex, AIC, and B4C absorbers in the assembly guide tubes, as well as position the RCCA by simply providing the number of steps withdrawn for the bank.

The reference cases for Problem 4 involve a series of different control rod positions. The first case has the bottom of the RCCA poison at a discrete position of 259.7 cm, relative to the top of the bottom core plate. This position is precisely between two spacer grids and is also an axial mesh boundary in the reference solution, and was chosen for being close to the critical position of Problem 5. The other eleven cases for Problem 4 for are for RCCA positions spacing fully inserted to fully withdrawn at 10% increments. From these cases, differential and integral control rod rods can be calculated and compared to the reference." – Ref. [1].

RESULTS

Table 8 provides the computed multiplication factor for the problem 4 scenarios for MCNPX and KENO, as well as the difference in [pcm]. Figure 23 provides the computed differential rod worth for both MCNPX and KENO, while Figure 24 provides the computed integral rod worth curve for MCNPX and KENO.

For a representative rod worth case, problem 4 with a 184 step RCCA insertion was run with 24 processors for a total of 17000 minutes CPU time [kcode 2e5 1.0 250 1500]. Only k_{eff} was computed, as no lattice tally was present for the rod worth cases. In contrast, problem 4 with a 167 step insertion ran on 150 cpus, consumed 66300 CPU minutes [kcode 5e5 1.0 250 2500] and was run with lattice tallies. The full pin power output is available in supporting files for this case. A 3D visualization of this data is shown in Figure 25. Details of the KENO reference calculations are included in Ref. [1].

The AMA benchmark specification requires problem 4 to be run at a continuous energy cross section temperature of 565K for the fuel and moderator. Hence NJOY 2012 was used to generate ENDF VII.0 565K ACE-formatted MCNPX libraries.

The MCNPX problem 3B result was corrected by -40 [pcm] to account for this study's use of 550K S(α,β) thermal scattering treatment of the H1 isotope. This was determined by interpolating between results obtained from using 550 and 600K light water S(α,β) libraries.

Table 8) Problem 4 MCNPX vs. KENO k_{eff} comparison (Table P4-4, p. 53, Ref [1]).

Rod Position [cm]	% Width-drawn	MCNPX 565K CE	Std dev	KENO 565K CE	Std dev	**Diff [pcm]**
259.7	-	0.99869	3.00E-05	0.998981	5.39E-06	-29.10
0	0	0.9721	4.00E-05	0.972411	1.48E-05	-31.10
23	10	0.9734	4.00E-05	0.973679	1.39E-05	-27.90
46	20	0.97899	4.00E-05	0.979363	1.58E-05	-37.30
69	30	0.98668	4.00E-05	0.987043	1.48E-05	-36.30
92	40	0.99201	4.00E-05	0.992341	1.39E-05	-33.10
115	50	0.99541	4.00E-05	0.995745	1.39E-05	-33.50
138	60	0.99773	4.00E-05	0.998028	1.48E-05	-29.80
161	70	0.99923	4.00E-05	0.999551	1.30E-05	-32.10
184	80	1.0003	4.00E-05	1.000584	1.30E-05	-28.40
207	90	1.00087	4.00E-05	1.001168	1.30E-05	-29.80
230	100	1.00113	4.00E-05	1.001385	1.30E-05	-25.50

Table 9) Differential Rod Worth Comparison.

Rod Position [cm]	**% Width-drawn**	**MCNPX DRW [pcm]**	**Std dev**	**KENO DRW [pcm]**	**Std dev**	**Diff [pcm]**
0	0	-137	8	-130	3.0	-7
23	10	-587	8	-582	3.0	-5
46	20	-796	8	-797	3.1	1
69	30	-545	8	-541	2.9	-4
92	40	-344	8	-347	2.8	3
115	50	-234	8	-226	2.9	-8
138	60	-150	8	-153	2.8	3
161	70	-107	8	-110	2.6	3
184	80	-57	8	-55	2.6	-2
207	90	-26	8	-29	2.6	3
230	100	-	-	-	-	-

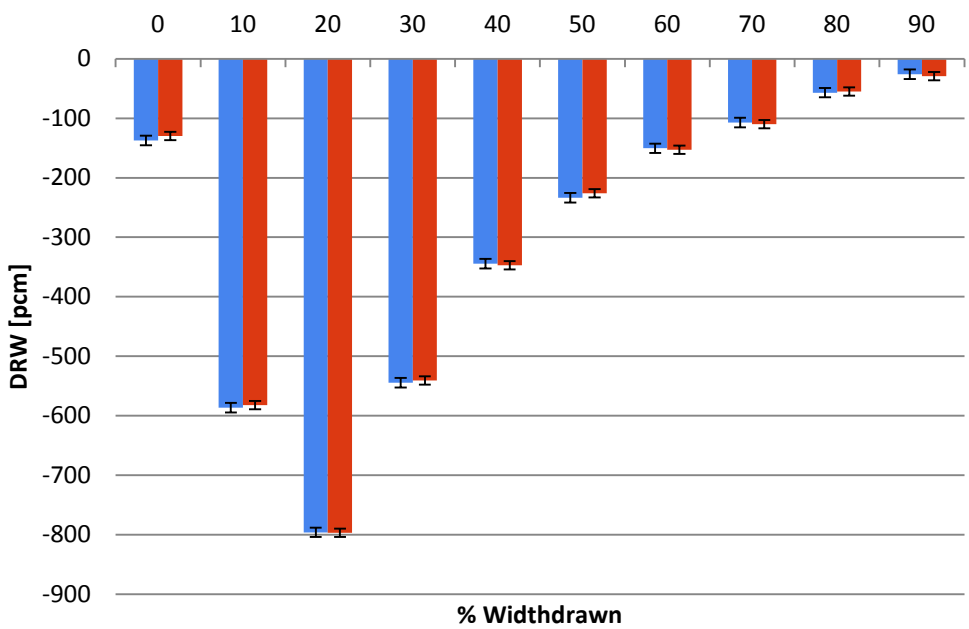

Figure 23) MCNPX (blue) vs. KENO (red) Differential Rod Worth for Problem 4.

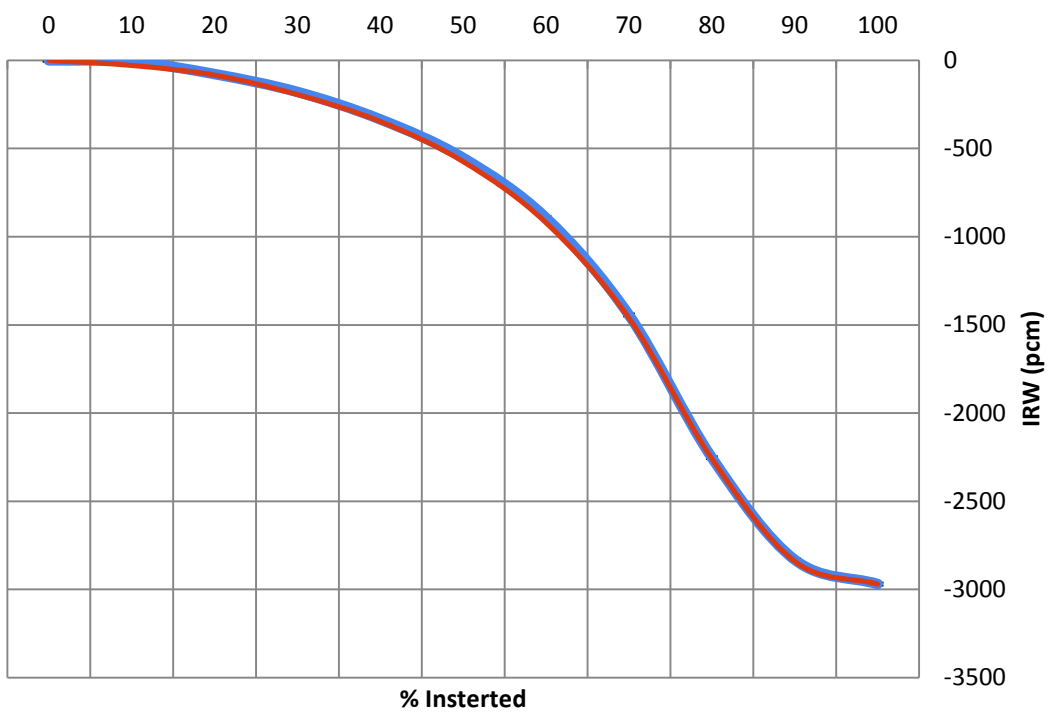

Figure 24) MCNPX (blue) vs. KENO (red) Integral Rod Worth for Problem 4. Uncertainty bars obscured by width of plotted lines.

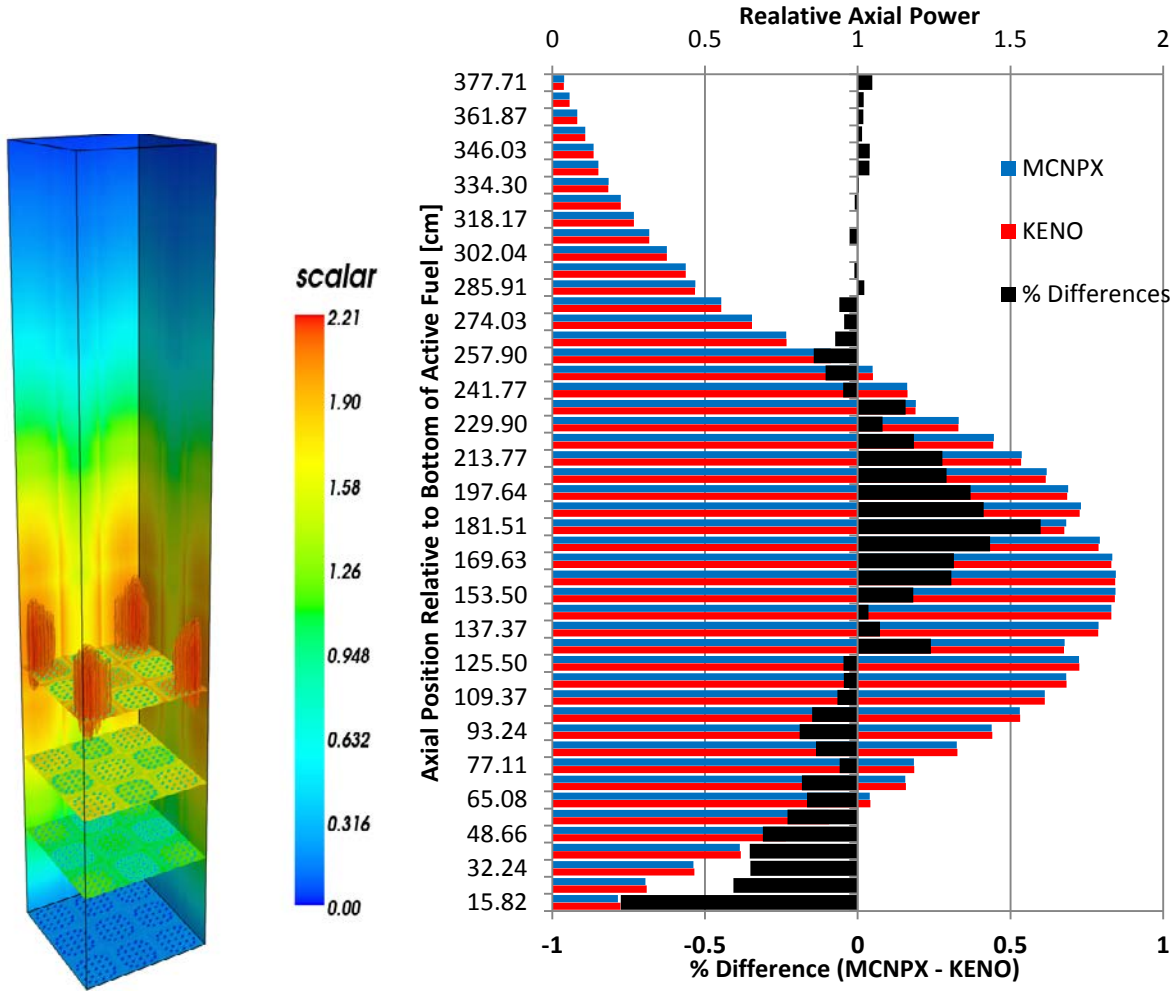

Figure 25) AMA P4 Pin power distribution. Control rods located 257.9 cm from bottom core plate. Right: Axial power distribution comparison with absolute percent difference shown.

A control rod has a bottom end plug that is defined to be 1.9 [cm] thick (Ref. [1]). In the MCNPX calculations, the bottom plane of the control rod is taken to be 15.131 [cm] from the top of the bottom core plate at full insertion.

The three-dimensional 3x3 assembly model allows for axial power distribution comparisons. The control rod bank position for this case is set to 257.9 cm from the bottom core plate. The absolute percent RMS axial power difference between the two codes for this case is 0.23%. A maximum absolute axial power difference of –0.77% occurs at bottom of the active fuel between MCNPX and KENO-VI. This case was run with 5e5 particles per generation for 2500 generations skipping 250 generations. This achieved an average axial power uncertainty of 0.32% with a maximum uncertainty of 1.12%.

For the 257.9 cm control rod bank insertion case for which pin powers tallies were set up, radial and assembly power distribution comparisons are possible. The assembly power comparison is presented in Figure 26. Assembly power results are in very good agreement.

KENO-VI

0.95571	
0.92490	1.08617

1 SD

0.001%	
0.001%	0.001%

MCNPX

0.95553	
0.92492	1.08620

0.365%	
0.331%	0.284%

% Diff

-0.0186%	
0.0019%	0.0027%

RMS **0.0066%**

Figure 26) Problem 4 167 step rod insertion assembly power plots.

PROBLEM #5: 3D HZP BOC QUARTER CORE

"The fifth AMA core physics benchmark progression problem expands the test suite to a full reactor model consistent with typical nuclear core analysis. Successful completion demonstrates the capability to predict the eigenvalue and core reactivity coefficients without thermal hydraulic feedback or depletion. The goal of this problem is to successfully perform the calculations associated with the Zero Power Physics Tests (ZPPT) that are performed at the beginning of each fuel cycle startup. The problem consists of a full core of Westinghouse 17x17-type fuel assemblies in the WBN1 initial loading pattern. All fuel is at beginning-of-life (BOL) and Hot Zero Power (HZP) isothermal conditions. In addition to the specification of Problem 4, this problem also tests the ability to define RCCA Banks and move them independently, and define and place incore instrumentation thimble tubes. This problem is ideally run in quarter symmetry, but the instrumentation does not have symmetry." – Ref. [1].

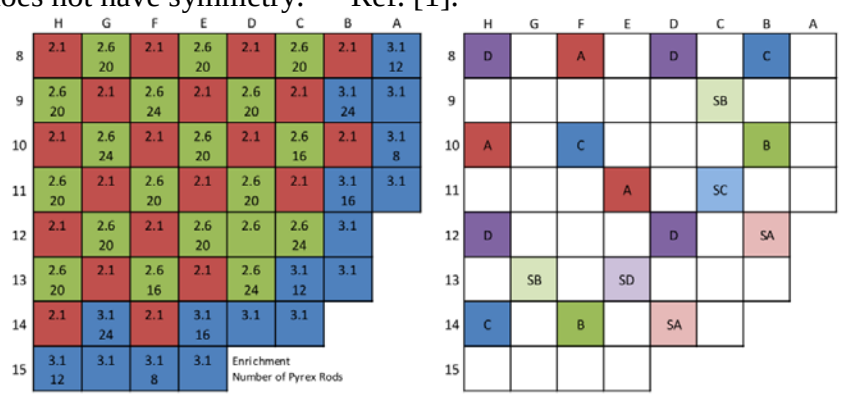

Figure 27) Top down view of WB1 quarter core model. RCCA bank positions shown on the right.

The reference cases for Problem 5 involve an investigation of a series of control rod bank positions, soluble boron concentrations, and temperatures to support the physics parameter calculations. The control rod bank positions are presented in Figure 27. The first case is a simulation of core critical with Bank D (regulating bank) at 167 steps withdrawn. This is the only problem 5-3D case for which pin powers were computed from fission rate tallies.

Bank positions relative to the bottom core plate are calculated by Equation (4).

$$Rod\ Position\ (cm) \ = \ 17.031 \ + \ (Nsteps \times 1.5875) \tag{4}$$

RESULTS

Problem 5 eigenvalue results are provided in Table 10. The mean eigenvalue difference for all problem 5 cases is -32.3 [pcm]. This is consistent with the reactivity bias seen in previous cases which involved far simpler geometry.

Table 10) Problem 5 eigenvalue only results.

Case	Boron [ppm]	Temp [K]	A	B	C	D	SA	SB	SC	SD	MCNPX keff +/- 2e-5	KENO keff +/-1e-5	Diff [pcm]
1	1285	**565**	-	-	-	**167**	-	-	-	-	0.999531	0.999899	-36.8
2	1291	↓	-	-	-	-	-	-	-	-	1.000041	1.000321	-28.0
3	1170	↓	**0**	-	-	**97**	-	-	-	-	0.998461	0.998797	-33.6
4	↓	↓	-	**0**	-	**113**	-	-	-	-	0.999041	0.999358	-31.7
5	↓	↓	-	-	**0**	**119**	-	-	-	-	0.998661	0.999039	-37.8
6	↓	↓	-	-	-	**18**	-	-	-	-	0.998801	0.999084	-28.3
7	↓	↓	-	-	-	**69**	**0**	-	-	-	0.998651	0.999022	-37.1
8	↓	↓	-	-	-	**134**	-	**0**	-	-	0.999041	0.999324	-28.3
9	↓	↓	-	-	-	**71**	-	-	**0**	-	0.998631	0.998983	-35.2
10	↓	↓	-	-	-	**71**	-	-	-	**0**	0.998621	0.998976	-35.5
11	↓	↓	-	-	-	-	-	-	-	-	1.012501	1.012841	-34.0
12	↓	↓	**0**	-	-	-	-	-	-	-	1.003421	1.003716	-29.5
13	↓	↓	-	**0**	-	-	-	-	-	-	1.003581	1.003941	-36.0
14	↓	↓	-	-	**0**	-	-	-	-	-	1.002491	1.002843	-35.2
15	↓	↓	-	-	-	**0**	-	-	-	-	0.998541	0.998815	-27.4
16	↓	↓	-	-	-	-	**0**	-	-	-	1.008011	1.008281	-27.0
17	↓	↓	-	-	-	-	-	**0**	-	-	1.001681	1.002018	-33.7
18	↓	↓	-	-	-	-	-	-	**0**	-	1.007331	1.007749	-41.8
19	↓	↓	-	-	-	-	-	-	-	**0**	1.007301	1.007745	-44.4
22	↓	↓	-	-	-	**0**	-	-	-	-	0.99244	0.992755	-31.5
23	↓	↓	-	-	-	**23**	-	-	-	-	0.99286	0.993162	-30.2
24	↓	↓	-	-	-	**46**	-	-	-	-	0.99425	0.994555	-30.5
25	↓	↓	-	-	-	**69**	-	-	-	-	0.99703	0.997369	-33.9
26	↓	↓	-	-	-	**92**	-	-	-	-	0.99999	1.000279	-28.9
27	↓	↓	-	-	-	**115**	-	-	-	-	1.00226	1.002542	-28.2
28	↓	↓	-	-	-	**138**	-	-	-	-	1.00387	1.004163	-29.3
29	↓	↓	-	-	-	**161**	-	-	-	-	1.00503	1.0053	-27.0
30	↓	↓	-	-	-	**184**	-	-	-	-	1.00575	1.006073	-32.3
31	↓	↓	-	-	-	**207**	-	-	-	-	1.00619	1.006468	-27.8
32	↓	↓	-	-	-	-	-	-	-	-	1.00630	1.006584	-28.4

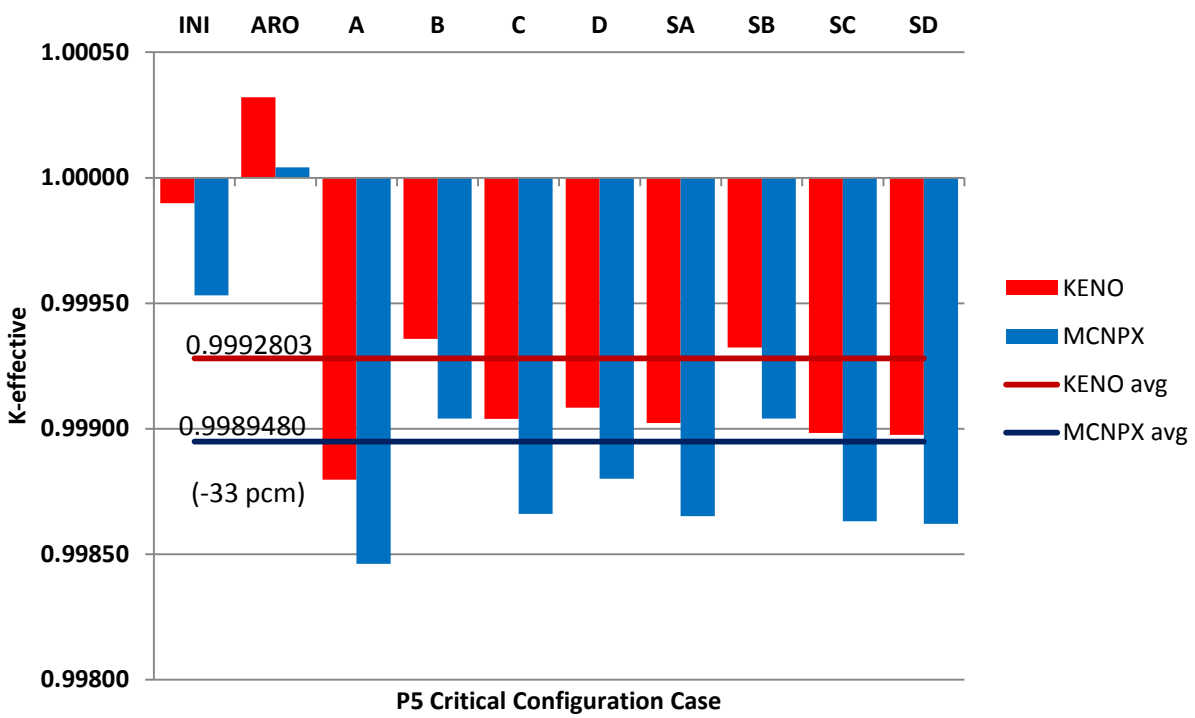

Figure 28) WB1 quarter core critical configuration summary plot.

Figure 28 depicts the critical configuration results from cases 1-10 in Table 10. The average difference in the eigenvalue results for problem 5 cases 1-10 is **-33 [pcm]**.

Isothermal Temperature Coefficient (ITC) experimental and numerical results for Watts Barr I are available. The ITC computation considers reactivity effects from Doppler broadening, thermal scattering, and moderator density changes. Isothermal temperature coefficient calculations are provided in Appendix A. The ITC results are summarized in Table 11.

Table 11) Problem 5 ITC results.

Case	MCNPX [pcm/K]	KENO [pcm/K]	Experiment [pcm/K]
MDC	-0.357± 0.075	-0.144± 0.036	-
DTC	-3.150± 0.285	-2.790± 0.036	-
S(α,β)	-2.860± 0.056	-2.790± 0.054	-
ITC	**-6.367± 0.416**	**-5.724± 0.072**	**-3.888**

Bank D rod worth results were generated for cases 22 – 32 of Table 10. The MCNPX and KENO bank D rod worth results agree within 10 [pcm] for every case.

Table 12) Problem 5 RCCA bank D differential rod worth comparison table.

Rod Position [cm]	% Width-drawn	MCNPX DRW [pcm]	Std dev	KENO DRW [pcm]	Std dev	Diff [pcm]
0	0	-10.9	4.0	-11.5	2.6	0.6
23	10	-43.5	4.0	-39.0	2.6	-4.5
46	20	-71.2	4.0	-76.4	2.8	5.2
69	30	-115.0	5.0	-112.6	2.7	-2.3
92	40	-160.0	5.0	-161.0	2.5	1.0
115	50	-226.5	4.0	-225.7	2.6	-0.8
138	60	-296.9	4.0	-291.7	2.7	-5.2
161	70	-280.5	4.0	-283.7	2.7	3.2
184	80	-140.8	4.0	-141.0	2.5	0.2
207	90	-42.6	4.0	-41.3	2.5	-1.3
230	100	-	-	-	-	-

Differential and integral rod worth plots are given in Figure 29 and Figure 30 respectively.

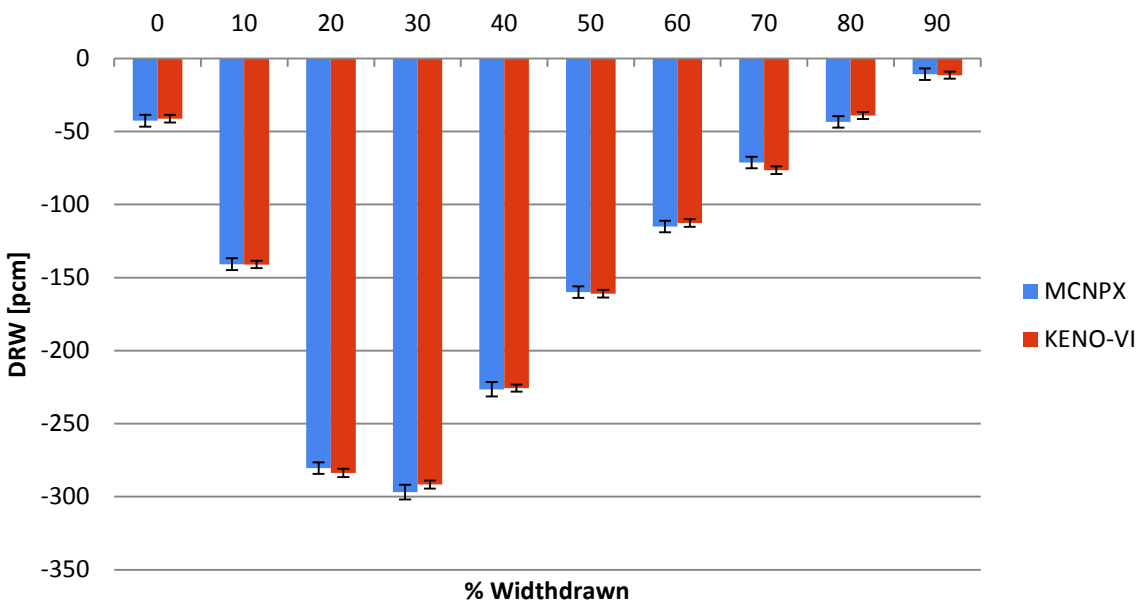

Figure 29. Differential rod worth curve for bank D in Watts Bar I 3D quarter core case.

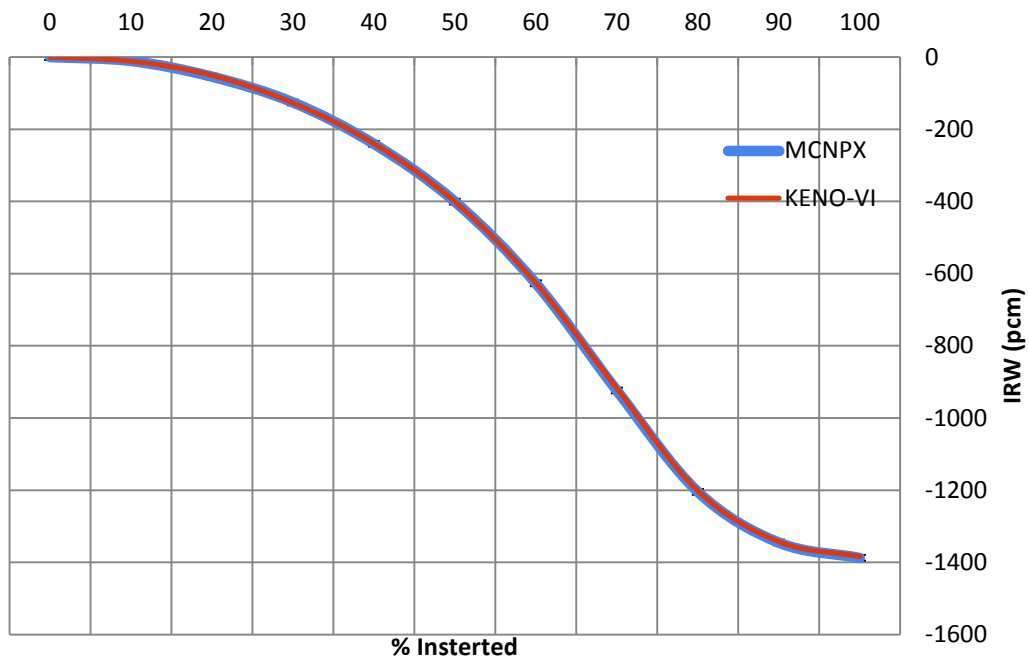

Figure 30. Integral rod worth curve for bank D in Watts Bar I 3D quarter core.

Total rod worth is presented for each RCCA bank in Table 13. Soluble boron concentration worth was computed from the all rods out configuration (cases p5-2 and p5-11). Rod worth in [pcm] is computed by Equation (5).

$$\rho = 1e5\left(\frac{1}{k_1} - \frac{1}{k_2}\right) \tag{5}$$

Table 13) Problem 5 ZPPT rod and boron worth results.

	MCNPX [pcm]	KENO [pcm]	MCNPX – KENO diff [pcm]	Measured [pcm]
Bank A	894	898	3.9	843
Bank B	878	875	-2.6	879
Bank C	986	984	-1.9	951
Bank D	1381	1386	5.7	1342
Bank SA	440	447	6.6	435
Bank SB	1067	1066	-0.4	1056
Bank SC	507	499	-8.0	480
Bank SD	510	499	-10.6	480
All Banks	6662	6655	-7.3	6467
Boron Worth [[pcm]/ppm]	-10.17	-10.21	0.04	-10.77

The rod bank worth differences are greatest for the shutdown banks SC and SD. Banks SC and SD are not arranged in quarter symmetry. From ref [1], a correction of **-53 [pcm]** was applied to the MCNPX calculated eigenvalues in which Bank SC or bank SD were fully inserted. Excellent soluble boron worth agreement is seen between the two codes.

Case 1, with a boron concentration of 1285 [ppm] and a bank D position of 167 steps withdrawn, was repeated with a pin power tally enabled. When compared to the eigenvalue-only calculation, a substantially larger number of particle histories were used to reduce the uncertainty in the pin power tallies, particularly in locations of low power. 2bn particle histories were run in MCNPX corresponding to a kcode of [1e6 1.0 500 2000]. This case was run on a single 64 cpu node with a wall time of 230 hours. Absolute axial power percent differences are given in Figure 31. A radial assembly power distribution comparison is made in Figure 32.

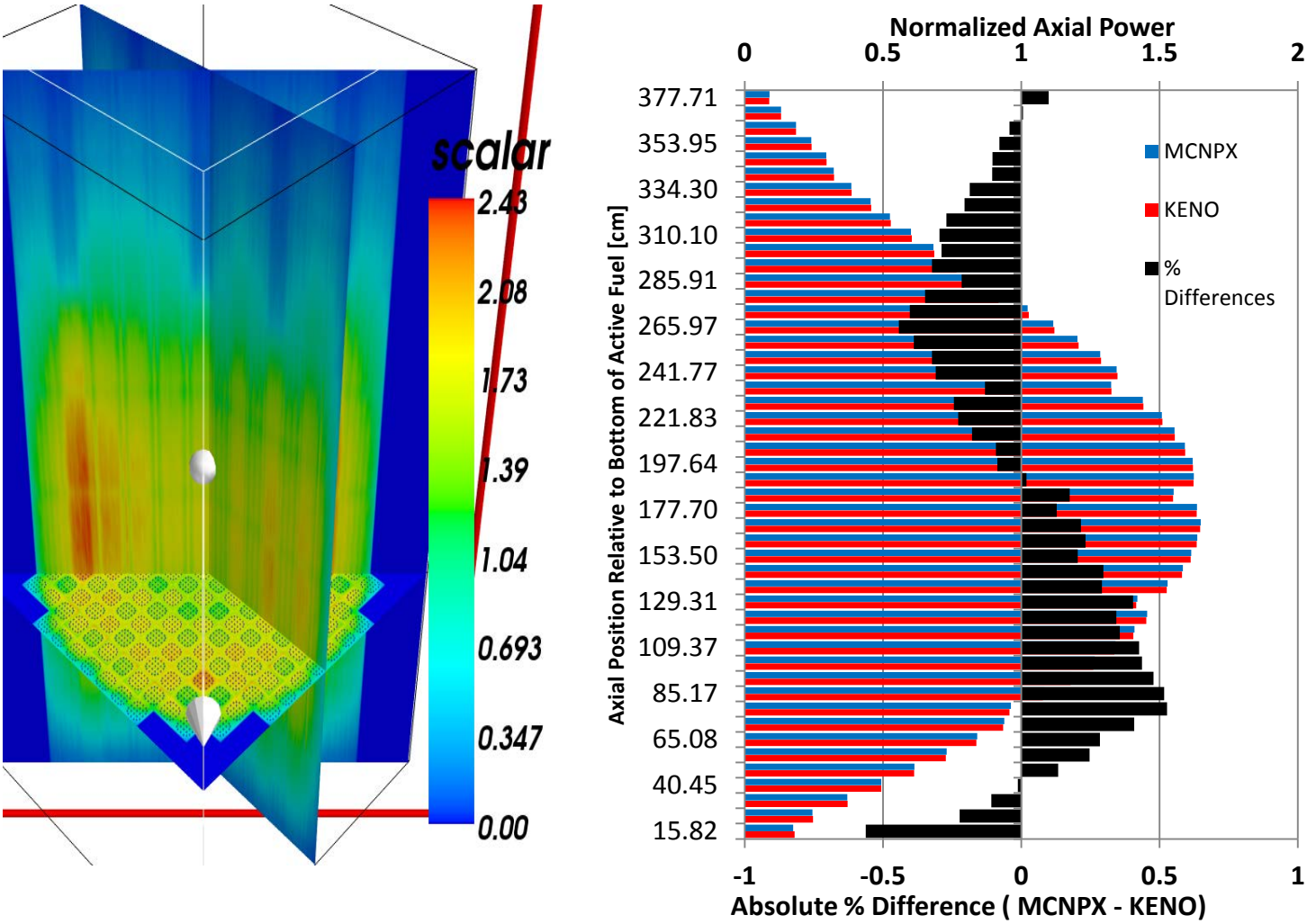

Figure 31) Left) Visualization of the 3D pin power distribution. Performed with Mayavi2. Right) Radially integrated, axial power distribution comparison between MCNPX and KENO-VI. All absolute axial percent differences are below 1.0%.

The axial percent RMS difference was found to be 0.135% between the MCNP and KENO result. Taking the KENO-VI result as truth, the sinusoidal axial error distribution indicates failure to completely converge the fission source distribution in MCNPX. Although the differences in question are small in magnitude, if computing resources were available running a larger number of particle histories would further reduce uncertainties and eliminate residual axial harmonics in the power distribution.

0.951	0.921	1.019	0.988	1.067	1.050	1.086	0.795
0.921	0.997	0.910	1.085	1.050	1.166	1.070	0.909
1.019	0.910	1.068	1.045	1.177	1.158	1.108	0.808
0.988	1.085	1.045	1.163	1.089	1.156	1.055	0.661
1.067	1.050	1.177	1.089	1.239	0.901	0.948	
1.050	1.166	1.158	1.156	0.901	0.915	0.630	
1.086	1.070	1.108	1.055	0.948	0.630		
0.795	0.909	0.808	0.661				

avg: 1.000 **min:** 0.630 **max:** 1.239

-0.09%	-0.15%	-0.23%	-0.04%	-0.13%	-0.15%	-0.08%	-0.09%
-0.15%	-0.32%	-0.09%	-0.02%	-0.04%	0.09%	0.17%	-0.10%
-0.23%	-0.09%	0.01%	0.08%	-0.06%	0.20%	0.04%	0.11%
-0.04%	-0.02%	0.08%	-0.17%	0.10%	0.18%	0.22%	-0.06%
-0.13%	-0.04%	-0.06%	0.10%	-0.19%	0.09%	-0.06%	
-0.15%	0.09%	0.20%	0.18%	0.09%	0.00%	-0.23%	
-0.08%	0.17%	0.04%	0.22%	-0.06%	-0.23%		
-0.09%	-0.10%	0.11%	-0.06%				

RMS: 0.133

Figure 32) Left) MCNPX Axially integrated assembly power distribution for the 3D-p5, case 1. Right) MCNPX – KENO assembly power distribution relative percent difference map.

Pin power percent differences are binned by KENO-VI average pin power standard deviations in Table 14. Nearly 63% of the MCNPX pin power cells are within 1 standard deviation of the KENO result.

Table 14) 3D pin power difference summary.

σ	# Cells	Cumulative % # Cells
1	394995	62.8%
2	185820	92.4%
3	41555	99.0%
4	5279	99.9%
5	704	100.0%
6	165	↓
7	46	↓
8	6	↓
9	2	↓

The overall quarter core pin power RMS percent difference is 1.050%. The average MCNPX pin power uncertainty for this model was 0.901%. A summary of the MCNPX pin power uncertainties is given in Table 15. Ideally, the maximum reported MCNPX pin power uncertainty (7.153%) should be reduced from its current value by a factor of 4 to bring the uncertainties in line with the KENO result, but this would require greater than an order of magnitude more particle histories to be run. This fidelity is not achievable on the available hardware at this time.

Table 15)MCNPX p5-3D pin power uncertainty summary.

Metric	Value
Avg 1σ PP	0.901%
Avg 1σ Axial	0.011%
Avg 1σ AsmRadial	0.009%
Max 1σ PP	7.153%

MISCELLANEOUS BENCHMARKS

Problem #4-2D: 2D HZP BOC 3x3 Assembly

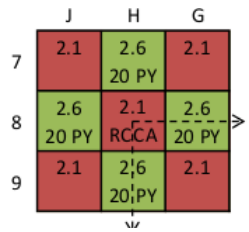

This problem is a simplification of problem #2. A 2D slice of a 3x3 array of assemblies is considered. The problem is run at a CE cross section temperature of 600 Kelvin.

As a representative example, problem 4-2D was run with 150 processors for a total of 18800 minutes CPU time [kcode 5e5 1.0 75 175] resulting in a 2.2 hour wall-time. Details of the KENO reference calculations are included in Ref. [1].

Table 16) MCNPX vs KENO k_{eff} comparison for problem 4-2D.

Case	MCNPX	sigma	KENO	sigma	diff [pcm]
4-2D Uncontrolled	1.00996	8.00E-05	1.01024	1.30E-05	-28
4-2D AIC-Controlled	0.98318	9.00E-05	0.983446	1.20E-05	-27

RMS Pin power differences are displayed in Table 17. Difference maps are also provided. The absolute color scale is defined such that a +0.5% relative error (MCNPX higher than KENO) gives a deep red and a -0.5% results yields a deep blue. The maximum and average relative MCNPX pin power uncertainty was 0.310% and 0.163% respectively for the controlled case. The plots do not indicate radial tilt or significant local reactivity bias due the presence of the B_4C rods in the controlled case.

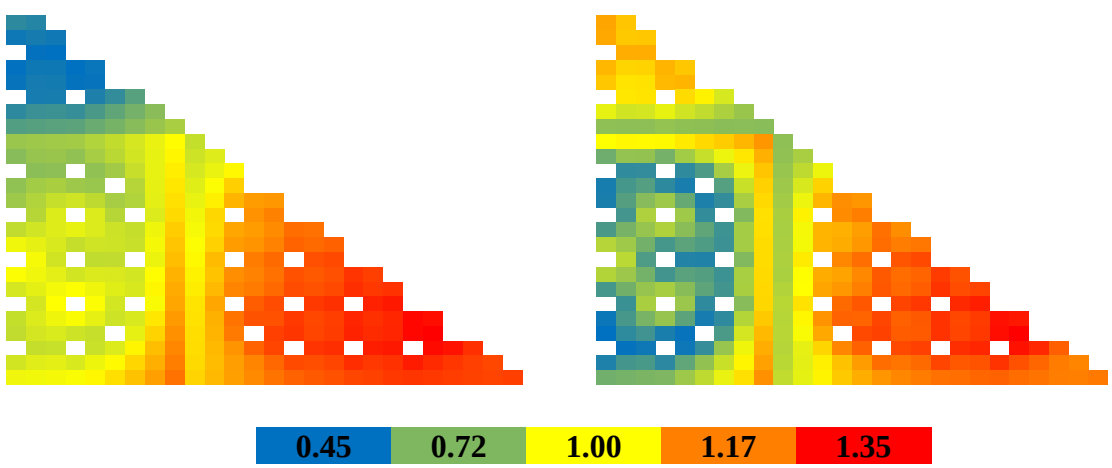

Figure 33) P4-2D pin power results. Left: AIC-Controlled. Right: Uncontrolled.

Table 17) MCNPX vs KENO-VI pin power %RMS differences for Problem 4-2D

Case	%RMS Difference
4-2D Uncontrolled	0.188%
4-2D Controlled	0.183%

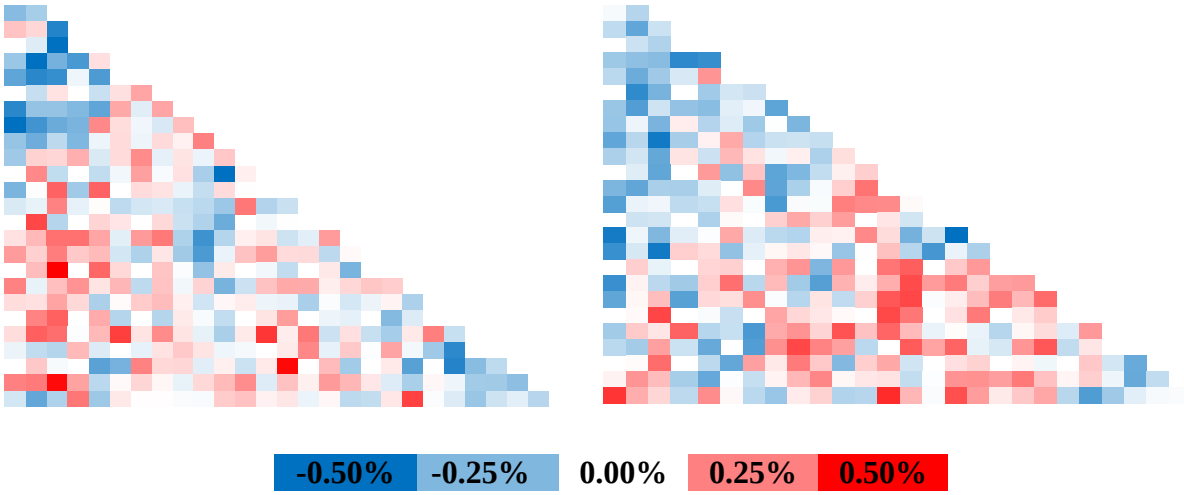

Figure 34) Octant symmetric MCNPX vs KENO-VI Pin Power %Difference maps.P4-2D Controlled on the left, P4-2D Uncontrolled on the right. A +0.5% [MCNP – KENO] relative error gives a deep red and a -0.5% result yields a deep blue.

MCNPX pin power uncertainty distributions are available in supporting files. A summary of the MCNPX pin power uncertainties for P4-2D are provided in Table 18.

Table 18) P4-2D MCNPX Pin power uncertainty summary

Case	Average %Uncert	Min %Uncert	Max %Uncert
4-2D Uncontrolled	0.159%	0.134%	0.255%
4-2D Controlled	0.163%	0.134%	0.310%

Normalized assembly powers are compared in Table 19 and Table 20. The normalized assembly power is computed by averaging the constitutive normalized pin powers in the assembly. Assembly power map comparisons are convenient and more succinct than a pin by pin comparison when the problem size increases beyond singe assemblies. Pin by pin comparisons generated by the VERAdiff utility may be found in supporting files.

Table 19) P4-2D Uncontrolled normalized assembly powers.

Assembly Powers

MCNP

0.99607	
0.92232	1.07866

1SD Uncert

0.163%	
0.169%	0.148%

KENO

0.99772	
0.92262	1.07795

0.004%	
0.003%	0.002%

%Diif

-0.166%	
-0.033%	0.066%

RMS 0.074%

Table 20) P4-2D Controlled normalized assembly powers.

Assembly Powers				
MCNP			**1SD Uncert**	
0.56930			0.209%	
0.92643	1.18125		0.171%	0.144%
KENO				
0.57019			0.006%	
0.92597	1.18148		0.003%	0.002%
%Diif				
-0.157%				
0.050%	-0.020%			
RMS	0.063%			

Problem #5-2D: 2D HZP BOC Quarter Core

This problem is a simplification of the 3D quarter core case. The simplified geometry reduces the computational requirement while remaining a valuable indicator of the ability of a code to predict detailed power distributions across a quarter core axial slice. In addition, the problem tests a code's ability to accurately predict pin power depression due to neutron leakage at the radial core boundary. This problem is run at a fuel and moderator temperature of 565K.

The uncontrolled and AIC-controlled P5-2D results were obtained running 2bn particle histories [kcode 1e6 1.0 600 2000] using 64 cores on a single compute node. The wall time for each P5-2D problem was 196 hours. Building on previous work carried out in the summer of 2014, UT-Austin consolidated pin power lattice tallies in order to improve the efficiency of the tally rendezvous process inside MCNPX. This improvement brought much reduced runtimes for this case. The B4C controlled computation included 2.5bn particle histories.

The S(α,β) scattering treatment of the H1 isotope bound to oxygen in water was evaluated at 550K due to data availability. The MCNPX and KENO-VI results are corrected by 42.5 [pcm] to account for this.

Table 21) P5-2D k_{eff} Result Summary.

Case	MCNPX	sigma	KENO	Sigma	diff [pcm]
5-2D Uncontrolled	1.003795	2.00E-05	1.004085	8.00E-06	-29
5-2D AIC Controlled	0.991255	2.00E-05	0.991496	8.00E-06	-24
5-2D B4C Controlled	0.989955	9.00E-05	0.990227	9.00E-06	-27

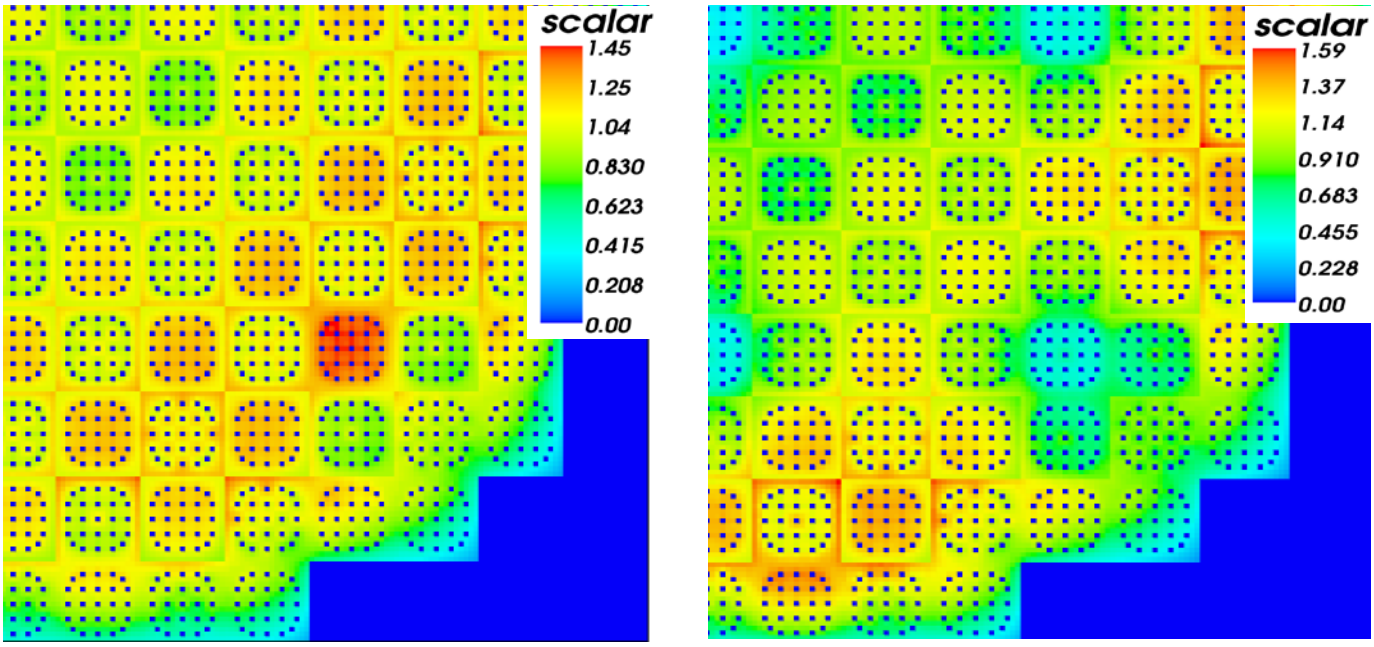

Figure 35) P5-2D pin power maps. Left: Uncontrolled case. Right: AIC controlled pin power distribution MCNPX result. Control bank D used. (Not pictured: B4C controlled pin power map).

The contrasting power distribution's shape between the uncontrolled and AIC-controlled cases is apparent in Figure 35. A summary of MCNPX pin power uncertainties for P5-2D is provided in Table 22. For each case, all MCNPX computed pin power uncertainties remain below 1%.

Table 22) P5-2D MCNPX Pin power uncertainty summary.

Case	Average %Uncert	Max %Uncert
5-2D Uncontrolled	0.14%	0.29%
5-2D AIC Controlled	0.14%	0.31%
5-2D B4C Controlled	0.12%	0.30%

Assembly power distributions are displayed in Figure 37, Figure 39 and Figure 41. Quarter symmetric assembly powers are weighted according to the map shown in Figure 36 when computing the RMS difference.

1.000	2.000	2.000	2.000	2.000	2.000	2.000	2.000
2.000	4.000	4.000	4.000	4.000	4.000	4.000	4.000
2.000	4.000	4.000	4.000	4.000	4.000	4.000	4.000
2.000	4.000	4.000	4.000	4.000	4.000	4.000	4.000
2.000	4.000	4.000	4.000	4.000	4.000	4.000	
2.000	4.000	4.000	4.000	4.000	4.000	4.000	
2.000	4.000	4.000	4.000	4.000	4.000		
2.000	4.000	4.000	4.000				

Figure 36) P5-2D Assembly power weights.

The assembly power distributions are simpler to visually compare than the large pin power maps. As elsewhere in this report, the maps report relative percent differences. The corresponding MCNPX uncertainties for each assembly power are presented in Figure 38, Figure 40 and Figure 42.

0.446	0.745	0.930	0.827	0.559	1.027	1.285	1.001
0.745	0.881	0.855	0.994	0.942	1.218	1.268	1.145
0.930	0.855	1.038	1.014	1.165	1.241	1.303	0.999
0.827	0.994	1.014	1.079	0.950	1.151	1.184	0.793
0.559	0.942	1.165	0.950	0.624	0.788	0.993	
1.027	1.218	1.241	1.151	0.788	0.854	0.639	
1.285	1.268	1.303	1.184	0.993	0.639		
1.001	1.145	0.999	0.793				

avg: 1.000 **min:** 0.446 **max:** 1.303

-0.54%	-0.50%	-0.50%	-0.33%	-0.19%	0.14%	0.14%	0.11%
-0.50%	-0.50%	-0.44%	-0.33%	-0.02%	0.09%	0.15%	0.10%
-0.50%	-0.44%	-0.32%	-0.09%	0.04%	0.11%	0.09%	0.10%
-0.33%	-0.33%	-0.09%	0.05%	0.10%	0.16%	0.14%	0.00%
-0.19%	-0.02%	0.04%	0.10%	0.04%	0.14%	0.13%	
0.14%	0.09%	0.11%	0.16%	0.14%	0.14%	0.09%	
0.14%	0.15%	0.09%	0.14%	0.13%	0.09%		
0.11%	0.10%	0.10%	0.00%				

RMS Er 0.21%

Figure 37) AIC Controlled assembly power distribution MCNPX result with a MCNPX vs KENO relative %difference map.

0.21%	0.17%	0.14%	0.16%	0.18%	0.14%	0.12%	0.16%
0.17%	0.14%	0.15%	0.13%	0.15%	0.12%	0.13%	0.15%
0.14%	0.15%	0.13%	0.14%	0.12%	0.13%	0.12%	0.16%
0.16%	0.13%	0.14%	0.13%	0.15%	0.12%	0.14%	0.18%
0.18%	0.15%	0.12%	0.15%	0.18%	0.16%	0.16%	
0.14%	0.12%	0.13%	0.12%	0.16%	0.17%	0.20%	
0.12%	0.13%	0.12%	0.14%	0.16%	0.20%		
0.16%	0.15%	0.16%	0.18%				

avg: 0.15% **min:** 0.12% max: 0.21%

Figure 38) MCNPX relative 1SD uncertainty in P5-2D controlled assembly powers

1.004	0.929	1.016	0.996	1.124	1.052	1.066	0.776
0.929	0.997	0.904	1.083	1.056	1.155	1.048	0.888
1.016	0.904	1.057	1.037	1.171	1.143	1.086	0.789
0.996	1.083	1.037	1.165	1.100	1.152	1.040	0.648
1.124	1.056	1.171	1.100	1.316	0.913	0.945	
1.052	1.155	1.143	1.152	0.913	0.923	0.631	
1.066	1.048	1.086	1.040	0.945	0.631		
0.776	0.888	0.789	0.648				

avg: 1.000 **min:** 0.631 **max:** 1.316

-0.19%	-0.16%	-0.07%	0.02%	-0.06%	0.02%	-0.11%	-0.11%
-0.16%	-0.23%	-0.10%	0.00%	0.05%	-0.02%	-0.03%	-0.02%
-0.07%	-0.10%	-0.03%	0.07%	0.07%	0.09%	0.04%	0.08%
0.02%	0.00%	0.07%	0.06%	0.10%	0.05%	0.07%	-0.04%
-0.06%	0.05%	0.07%	0.10%	0.06%	-0.01%	-0.02%	
0.02%	-0.02%	0.09%	0.05%	-0.01%	-0.10%	-0.14%	
-0.11%	-0.03%	0.04%	0.07%	-0.02%	-0.14%		
-0.11%	-0.02%	0.08%	-0.04%				

RMS Err: 0.08%

Figure 39) Uncontrolled assembly power distribution MCNPX result alongside a MCNPX vs KENO relative %difference map.

0.14%	0.15%	0.13%	0.14%	0.13%	0.14%	0.13%	0.18%
0.15%	0.13%	0.15%	0.13%	0.14%	0.12%	0.14%	0.17%
0.13%	0.15%	0.13%	0.14%	0.12%	0.13%	0.13%	0.17%
0.14%	0.13%	0.14%	0.13%	0.13%	0.12%	0.15%	0.20%
0.13%	0.14%	0.12%	0.13%	0.13%	0.15%	0.16%	
0.14%	0.12%	0.13%	0.12%	0.15%	0.16%	0.20%	
0.13%	0.14%	0.13%	0.15%	0.16%	0.20%		
0.18%	0.17%	0.17%	0.20%				

avg: 0.15% **min:** 0.12% max: 0.20%

Figure 40) MCNPX relative 1SD uncertainty in P5-2D Uncontrolled assembly powers

0.399	0.726	0.921	0.807	0.506	1.021	1.310	1.028
0.726	0.869	0.849	0.984	0.927	1.224	1.293	1.175
0.921	0.849	1.036	1.009	1.163	1.252	1.328	1.024
0.807	0.984	1.009	1.066	0.930	1.149	1.200	0.811
0.506	0.927	1.163	0.930	0.558	0.773	0.999	
1.021	1.224	1.252	1.149	0.773	0.845	0.639	
1.310	1.293	1.328	1.200	0.999	0.639		
1.028	1.175	1.024	0.811				

0.12%	0.20%	0.15%	0.09%	-0.18%	-0.10%	-0.05%	-0.12%
0.20%	0.13%	0.12%	0.07%	0.05%	-0.06%	0.00%	-0.15%
0.15%	0.12%	0.09%	0.10%	0.11%	0.03%	-0.05%	-0.12%
0.09%	0.07%	0.10%	0.12%	0.07%	0.00%	0.01%	-0.08%
-0.18%	0.05%	0.11%	0.07%	-0.10%	-0.02%	-0.01%	
-0.10%	-0.06%	0.03%	0.00%	-0.02%	-0.08%	-0.18%	
-0.05%	0.00%	-0.05%	0.01%	-0.01%	-0.18%		
-0.12%	-0.15%	-0.12%	-0.08%				

avg: 1.000 **min:** 0.399 **max:** 1.328 **RMS Er** 0.10%

Figure 41) B4C Controlled assembly power distribution MCNPX result with a MCNPX vs KENO relative %difference map.

0.15%	0.13%	0.13%	0.12%	0.13%	0.11%	0.12%	0.13%
0.20%	0.15%	0.13%	0.14%	0.16%	0.13%	0.11%	0.14%
0.15%	0.13%	0.13%	0.12%	0.13%	0.11%	0.12%	0.13%
0.13%	0.13%	0.12%	0.12%	0.11%	0.11%	0.10%	0.14%
0.14%	0.12%	0.12%	0.12%	0.13%	0.11%	0.12%	
0.16%	0.13%	0.11%	0.13%	0.17%	0.14%	0.14%	
0.13%	0.11%	0.11%	0.11%	0.14%	0.15%		
0.11%	0.12%	0.10%	0.12%				

avg: 0.13% **min:** 0.10% max: 0.20%

Figure 42) MCNPX relative 1SD uncertainty in P5-2D B4C controlled assembly powers.

The assembly power RMS differences are summarized in Table 23.

Table 23) Problem 5-2D Assembly power distribution relative RMS percent difference

Case	RMS % difference
5-2D Uncontrolled	0.08%
5-2D AIC Controlled	0.21%
5-2D B4C Controlled	0.10%

No radial tilt is seen in the uncontrolled comparison. A small degree of tilt is seen in the AIC-controlled case despite the same number of particle histories being run. The 2D single assembly case result presented in Figure 8 depicts apparent reactivity bias introduced by the AIC control absorber material. This same bias may contribute to the inward tilt of the MCNPX result when compared to the KENO result. Some degree of radial tilt is exhibited in the B4C controlled case, however, the radial assembly relative RMS percent difference remains less than 0.1%.

APPENDIX A

Problem #5 – 3D Quarter Core ITC Calculations

The reactivity sensitivity with respect to S(α,β) H1 temperature is shown in Table 24. A slight discrepancy between the Boron concentration used for ITC calculations between the MCNPX and KENO calculations is known to exist. KENO ITC calculations were performed with a Boron concentration of **1299 [ppm].** MCNPX ITC calculations were performed with a Boron concentration of **1291 [ppm]** as indicated in Table 10. As determined by comparing KENO results for cases P5-2 and P5-11, an **8 [ppm]** boron concentration difference was computed to be worth **83 [pcm].** This correction is applied to all results in Appendix A. The S(α,β) sensitivity calculations were performed with all rods withdrawn from the core.

Table 24) Problem 5 S(α,β) worth results.

Case	MCNPX	1SD	KENO	1SD	Diff [pcm]
S(α,β) 550 K	0.99963	2e-5	0.999876	1e-5	-23
S(a,b) 600 K	0.99820	2e-5	0.998485	1e-5	-28

Derivative information is provided in Table 25.

Table 25) Sensitivity of the eigenvalue to thermal scattering treatment of the H1 isotope in light water.

	MCNPX	1SD	KENO	1SD
565K S(a,b) slope [pcm/K]	-2.86	0.056	-2.78	0.054

MCNPX computations with slight perturbations to the moderator density due to small changes in temperature about 565 K were performed. The Moderator Density Coefficient (MDC) was computed by evaluating the derivative of a quadratic fit to the data at 565 K.

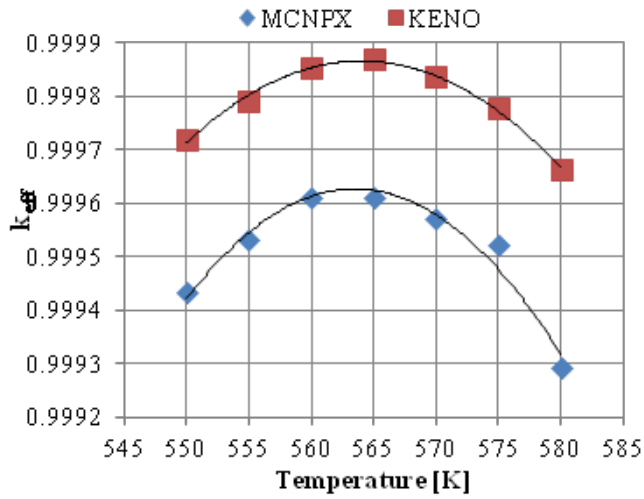

Figure 43) Moderator density only effect on keff.

Table 26) Moderator density coefficient

	MCNPX	1SD	KENO	1SD
565K MDC [pcm/K]	-0.357	0.075	-0.144	0.036

The Doppler Broadening Coefficient (DTC) is computed by utilizing Doppler broadened CE cross section libraries generated in NJOY 2012 at the indicated temperatures in MCNPX. In the DTC computations, all material free gas thermal scattering temperatures were set to the value used in the NJOY Doppler broadening routine and the S(α,β) H1 temperature is fixed at 550 K. The uncertainty in this coefficient is computed by the same method used to determine the moderator density coefficient uncertainty.

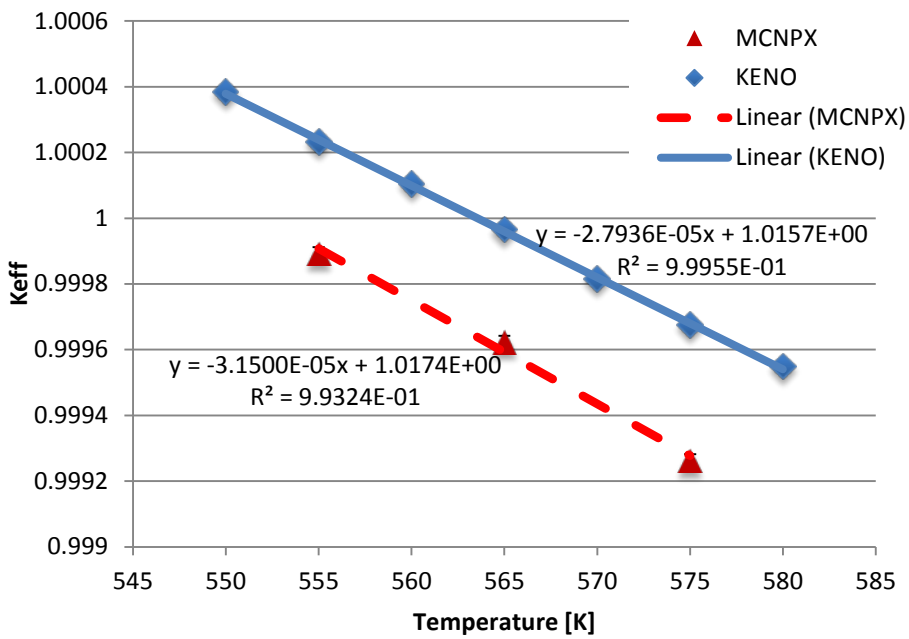

Figure 44) Doppler broadening effect on keff.

Table 27) Doppler temperature coefficient.

	MCNPX	1SD	KENO	1SD
565K DTC [pcm/K]	-3.150	0.285	-2.790	0.054

The uncertainties of the MDC and DTC derivatives were computed by Monte Carlo methods. At each Monte Carlo iteration, all data points were randomly sampled from a normal distribution with the standard deviation given by the MCNPX simulation results. The polynomial fits were reapplied and the derivatives at 565K recomputed. The standard deviation of the derivatives after 50,000 Monte Carlo iterations is reported.

An investigation regarding an apparent nonlinear relationship between the neutron multiplication factor and Doppler temperature in the MCNPX result was carried out. The KENO result in Figure 44 clearly shows a linear relationship. A plot of the old DTC result (circa September 2014) and the updated DTC result (January 2015) is shown in Figure 45.

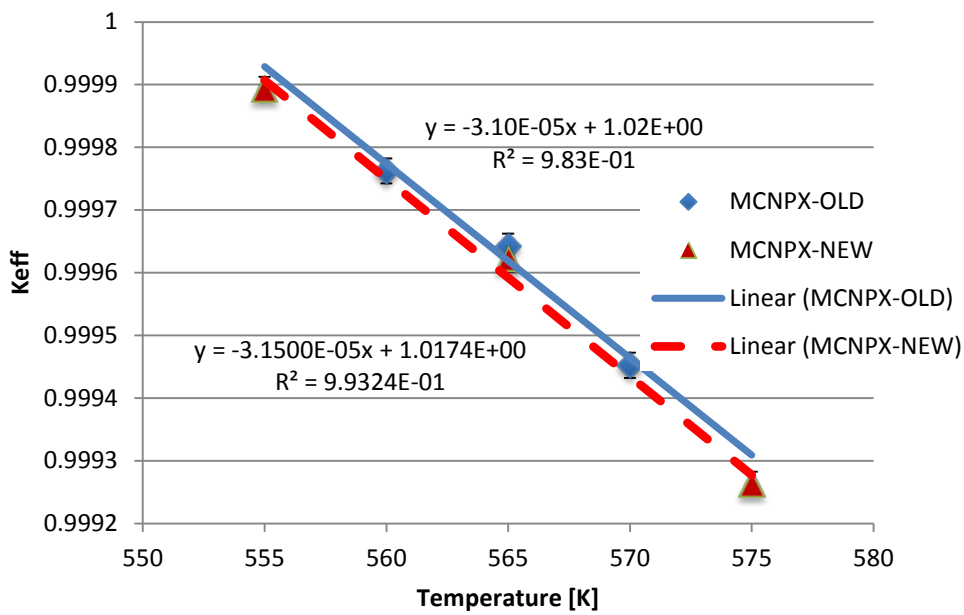

Figure 45) Refined DTC result compared to previous calculation.

Kcode old: [1e6 1.0 300 1000]. Kcode new: [1e6 1.0 500 2000]. The number of total particle histories was doubled from 1bn to 2bn. The R^2 statistic for a linear regression improved to 0.993 from 0.983. No significant difference in the slope computed at 565K was found. The updated DTC estimate is -3.15 [pcm/K]. The updated DTC is within 0.175σ of the previous result.

APPENDIX B

Pin Power Normalization

Pin power is a normalized fission reaction rate. The normalization is performed such that for the full core, the axial linear power [Power/m] profile averages to one.

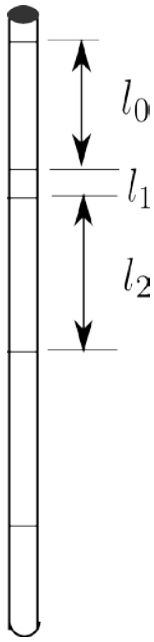

Assuming each rod has the same radius:

$$\overline{T_w} = \frac{1}{N}\sum_{i=0}^{N} l_i\, T_i$$

Where $\overline{T_w}$ is the weighted average tally value with weights given by the length of each tally axial segment length, l_i. N is the total number of axial segments. T_i is the raw reaction rate f4 tally value from MCNPX. The normalized pin powers are then computed:

$$P_i = \frac{T_i}{\overline{T_w}}$$

Where P_i is the pin power for a given axial fuel segment.

REFERENCES

[1] A. GODFREY, "VERA Core Physics Benchmark Progression Problem Specifications, Revision 3," Consortium for Advanced Simulation of LWRs, Oak Ridge National Laboratory, March 2013